



8-2000

Application of the electrostatic separation of recoil atoms to the ^{225}Ac - ^{221}Fr - ^{217}At - ^{213}Bi decay series

John Daniel Marsh

Follow this and additional works at: https://trace.tennessee.edu/utk_graddiss

Recommended Citation

Marsh, John Daniel, "Application of the electrostatic separation of recoil atoms to the ^{225}Ac - ^{221}Fr - ^{217}At - ^{213}Bi decay series. " PhD diss., University of Tennessee, 2000.
https://trace.tennessee.edu/utk_graddiss/8344

This Dissertation is brought to you for free and open access by the Graduate School at TRACE: Tennessee Research and Creative Exchange. It has been accepted for inclusion in Doctoral Dissertations by an authorized administrator of TRACE: Tennessee Research and Creative Exchange. For more information, please contact trace@utk.edu.

To the Graduate Council:

I am submitting herewith a dissertation written by John Daniel Marsh entitled "Application of the electrostatic separation of recoil atoms to the ^{225}Ac - ^{221}Fr - ^{217}At - ^{213}Bi decay series." I have examined the final electronic copy of this dissertation for form and content and recommend that it be accepted in partial fulfillment of the requirements for the degree of Doctor of Philosophy, with a major in Chemistry.

George K. Schweitzer, Major Professor

We have read this dissertation and recommend its acceptance:

Joe Peterson, John Turner, Larry Miller, Saed Mirzadeh

Accepted for the Council:

Carolyn R. Hodges

Vice Provost and Dean of the Graduate School

(Original signatures are on file with official student records.)

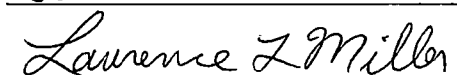
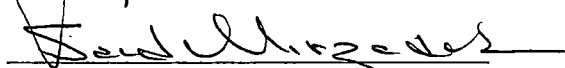
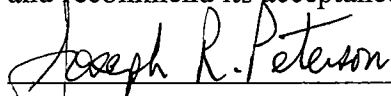
To the Graduate Council:

I am submitting here the dissertation written by J. Daniel Marsh entitled "The Application of the Electrostatic Separation of Recoil Atoms to the ^{225}Ac - ^{221}Fr - ^{217}At - ^{213}Bi Decay Series." I recommend that it be accepted in partial fulfillment of the requirements for the degree of Doctor of Philosophy, with a major in Chemistry.

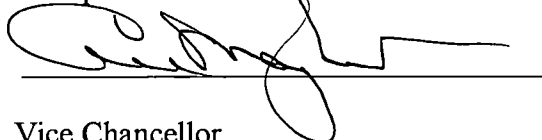


George K. Schweitzer, Major Professor

I have read this dissertation
and recommend its acceptance:



Accepted for the Council:



Vice Chancellor
Graduate Studies and Research

APPLICATION OF THE ELECTROSTATIC SEPARATION
OF RECOIL ATOMS
TO THE ^{225}Ac - ^{221}Fr - ^{217}At - ^{213}Bi DECAY SERIES

A Dissertation
Presented for the
Doctor of Philosophy
Degree
The University of Tennessee, Knoxville

J. Daniel Marsh

August 2000

Copyright © by J. Daniel Marsh, 2000

All Rights Reserved

DEDICATION

The author would like to dedicate this work to his wonderful wife, Peggy, and their children, John, Benjamin, Adair, David, and Brian, whose love, understanding, patience, and encouragement allowed him to accomplish this goal.

The author would also like to dedicate this work to his parents, John D. and Elizabeth S. Marsh, for fostering my love of science and allowing me to pursue my dreams.

ACKNOWLEDGMENT

The success of any dissertation is highly dependent on the advice, enthusiasm, leadership, and encouragement of the student's major professor. In this task, Dr. George K. Schweitzer excelled. I will never forget his lecture to me on the three types of logic: Inductive, Deductive, and Seductive. It was a very valuable lesson. To him, the author wishes to express his sincere gratitude and deepest appreciation.

The other person to whom this research owes much is Dr. Saed Mirzadeh of the Nuclear Medicine Group at Oak Ridge National Laboratory. His guidance and consultation were invaluable. He also provided the laboratory space and the resources that made this research possible.

The author would also like to thank the other members of his graduate committee, Dr. Joe Peterson, Dr. John Turner, and Dr. Larry Miller, for taking their valuable time to review this dissertation.

There are also numerous other people to whom thanks are due. Dr. Rose Boll prepared the ^{225}Ac sources, Arnold Beets shared his office and took care of my solid and liquid lab wastes, Anne Smalley took messages, reserved rooms, and was always pleasant to talk to, Lauren Larsen provided encouragement over the years, and my wife Peggy and eldest son John acted as editors and kept all the figures and tables straight. I'd also like to thank my other children Benjamin, Adair, David and Brian for offering encouragement and understanding when I was busy or needed to go to the lab on weekends or holidays and for picking up the slack in duties around the house. I'd also like to thank my wife again for being there for me during the tough times and for always believing in me.

ABSTRACT

The focus of this research was to develop a novel approach for the separation of ^{221}Fr and ^{213}Bi from ^{225}Ac . First a method was developed to electrodeposit the actinium onto a cathode from a pH = 2 nitric acid solution. Yields for the electrodeposition approached 99% for a one hour deposition. The Joliot Equation was used to quantitate the process. A linear velocity constant of 0.23 cm/min was measured for the electrodeposition of ^{225}Ac on a Pt electrode.

To separate the ^{221}Fr and ^{213}Bi , the atoms were caught in an electrostatic field as they recoiled from the cathode. The collection yield was found to be dependent on the electrostatic field strength with a critical voltage of about 2000 volts, above which the yield leveled off. The maximum yields for ^{221}Fr were found to occur after 40 minutes of collection. The yield for ^{221}Fr approached 50% while that for ^{213}Bi approached 99%.

It was found that the activity of ^{221}Fr on the collector plate could be calculated by multiplying the chain decay equation by a geometry correction factor of the form:

$$f = 0.5(1 - \cos\theta)$$

$$\text{where } \theta = \tan^{-1}(R/d)$$

and R = the radius of the collector and d is the distance between the plates. If secular equilibrium is assumed, then the equation reduces to simply: $A_{\text{Fr}} = A_{\text{Ac}} * f$.

The collection of the recoil atoms of ^{221}Fr and ^{213}Bi in an electrostatic field has been shown an effective and efficient means of their separation from ^{225}Ac .

TABLE OF CONTENTS

CHAPTER	PAGE
I. INTRODUCTION.....	1
A. Research Topic.....	1
B. Importance to Nuclear Medicine.....	3
II. PRODUCTION AND DECAY SCHEMATICS OF THE NEPTUNIUM SERIES.....	5
III. HISTORICAL INFORMATION.....	13
IV. SOURCE PREPARATION BY EVAPORATION.....	18
V. A SUMMARY OF ACTINIUM SOLUTION CHEMISTRY.....	22
VI. THE ELECTRODEPOSITION OF ACTINIUM.....	26
VII. THE ATOM RECOIL COLLECTOR (ARC).....	42
VIII. CALCULATION OF ACTIVITIES ON THE RECOIL COLLECTOR.....	64
IX. FUTURE WORK.....	67
X. SUMMARY AND CONCLUSIONS.....	70
LIST OF REFERENCES.....	72
APPENDICES.....	77
APPENDIX I. Source Solution Preparation.....	78
APPENDIX II. Electrodeposition Procedure.....	79
APPENDIX III. Atom Recoil Collection (ARC) Procedure.....	80
VITA.....	81

LIST OF TABLES

TABLE	PAGE
I. ENERGY COMPARISON OF SEPARATION TECHNIQUES.....	2
II. MAJOR GAMMA CHARACTERISTICS OF ^{225}Ac , ^{221}Fr , AND ^{213}Bi	9
III. SHELF EFFICIENCIES.....	10
IV. RECOIL ENERGIES OF THE ISOTOPES.....	14
V. PARAMETERS AND CONCENTRATIONS OF IMPURITIES IN ULTRAPURE NITRIC ACID.....	19
VI. CALCULATED RANGES FOR ^{221}Fr IN DIFFERENT MATRICES.....	21
VII. COMPLEX FORMATION CONSTANTS OF ACTINIUM WITH CHLORIDE AND NITRATE.....	25
VIII. YIELD CALCULATION FOR ELECTRODEPOSITION.....	33
IX. ACTIVITY OF ^{225}Ac IN SOLUTION AND AFTER ELECTRODEPOSITION AT PROGRESSIVE TIME INTERVALS.....	34
X. ACTINIUM ELECTRODEPOSITION RATE DATA	39
XI. CALCULATION OF ζ , η AND κ	40
XII. ^{221}Fr ATOM RECOIL COLLECTOR (ARC) CALCULATIONS.....	45
XIII. ^{213}Bi ATOM RECOIL COLLECTOR (ARC) CALCULATIONS.....	46
XIV. YIELD VS. VOLTAGE.....	48
XV. YIELD VS. TIME.....	50
XVI. YIELD VS. DISTANCE.....	53

TABLE	PAGE
XVII. YIELD VS. ELECTROSTATIC FIELD INTENSITY.....	56
XVIII. CALCULATION OF ^{221}Fr YIELD AFTER RECOIL COLLECTION.....	60
XIX. CALCULATION OF YIELD FOR ^{213}Bi AFTER RECOIL COLLECTION...	61

LIST OF FIGURES

FIGURE	PAGE
1. The Neptunium (4n+1) Series.....	6
2. Decay energies of the Neptunium (4n+1) Series.....	7
3. Efficiency curves for gamma-X detector.....	11
4. Pourbaix diagram for actinium.....	23
5. Gamma spectrum of ^{225}Ac solution prior to electrodeposition showing the presence of ^{225}Ac at 188 keV.....	29
6. Gamma spectrum of ^{225}Ac solution after electrodeposition showing the absence of ^{225}Ac at 188 keV.....	30
7. Decrease of ^{225}Ac in solution during electrodeposition.....	31
8. Increase of ^{225}Ac on cathode during electrodeposition.....	32
9. ^{221}Fr activity on cathode after electrodeposition.....	36
10. ^{213}Bi ingrowth on cathode after electrodeposition.....	37
11. Diagram of atom recoil collector showing lines of force between plates.....	43
12. % Yield vs. duration of recoil collection.....	49
13. % Yield vs. voltage.....	51
14. % Yield vs. voltage at constant ξ	54
15. % Yield vs. electrostatic field intensity.....	55
16. % Yield vs. distance between plates.....	57
17. Geometry factor diagram.....	59

FIGURE	PAGE
18. Gamma spectrum of cathode after recoil separation showing ^{221}Fr and ^{213}Bi collected.....	62
19. Gamma spectrum of cathode after recoil separation showing the absence of ^{225}Ac and the decay of ^{221}Fr and ^{213}Bi	63
20. ^{221}Fr Activity Measured vs. Calculated.....	66

LIST OF SYMBOLS

ARC the atom recoil collector

k the Boltzman Constant

T temperature in Kelvin

λ the decay constant of an isotope

ξ the electrostatic field strength

E_R the recoil energy of a daughter atom

E_α the alpha particle energy

M_α the mass of the alpha particle

M_R the mass of the recoil nucleus

A the mass number of the parent atom

ppb parts per billion

R_0 the range of a particle in a stopping medium

M_i the mass of an atom or ion

Z_i the atomic number of an atom

ρ density

$t_{1/2}$ the half-life of an isotope

E, E^0 the electrode and standard electrode potential, respectively

n the number of electrons taking part in a reaction

α the deposition velocity constant

β the dissolution velocity constant

N the number of atoms of ^{225}Ac electrodeposited on the cathode

N_0 the number of atoms of ^{225}Ac in the initial solution prior to electrodeposition

LIST OF SYMBOLS (Continued)

- ℓ a unitless proportionality constant in the Joliot Equation
- ϑ the deposition/dissolution constant in units of min^{-1} in the Joliot Equation
- κ the linear velocity constant
- dps disintegrations per second
- μCi microCurie – a unit of radioactivity
- ϵ_0 the permittivity of free space
- ϵ the product of K and ϵ_0
- K the dielectric constant
- F the force exerted on a particle by the electrostatic field
- C the capacitance between the collection plates
- Q the total charge on the capacitor
- V the potential difference between the cathode and the recoil collector or the volume of the initial solution. See context for meaning.
- A refers to either the area of the cathode or the area of the recoil collector. See context for meaning.
- $A_{\text{Fr}}, A_{\text{Ac}}$ the activity of ^{221}Fr and ^{225}Ac , respectively
- f the geometric correction factor
- θ the angle subtended between the source (cathode) and the recoil collector
- d the distance between the cathode and the recoil collector or the plates of a capacitor
- R the radius of the recoil collector
- RE_{max} the maximum recoil energy imparted by a beta particle
- E_{β} the maximum beta energy or beta max

CHAPTER I

INTRODUCTION

A. Research Topic

The purpose of this doctoral research was to devise a novel method of separation of the radionuclides ^{221}Fr (^{213}Bi) from ^{225}Ac . Previous separation schemes used ion exchange where the actinium was loaded onto an anion exchange resin and then, after sufficient ingrowth, the ^{213}Bi was eluted. However, because of the heat and radiation damage produced from the high specific activity of actinium and its daughters, the resin, in rather short time (a few days), is fused to the point where the column is no longer functional. This short shelf life of the column and the continuous production of milliCurie levels of radioactive wastes necessitated a new approach to the problem.

Two possible techniques were considered. They were collection of daughter recoil atoms in an electrostatic field and thermal evaporation of the francium atoms in equilibrium with an actinium source. The second technique is based on the very low boiling point for francium (677°C) compared with its parent actinium (3200°C). This second technique has been investigated and has become the subject of a masters thesis. [1] The first technique was based on the idea of Dr. Harvey Gould. [2] An analysis of the energies involved is given in Table I (p. 2). These calculations are based on the mass of ^{225}Ac , a temperature of 700°C and an electrostatic potential of 5000 volts. It

TABLE I.
ENERGY COMPARISON OF SEPARATION TECHNIQUES

Process	Energy of Process (keV)	Condition
Recoil	100	Mass Ac = 225 amu
Electrostatic Field	5	Applied Potential = 5000V
Thermal, kT	8.387E-05	T = 700°C

is obvious that the most energy available for separation comes from the recoil effect. However, as will be shown later, the application of an electrostatic field will greatly enhance this effect.

To collect the recoil atoms, a very thin source is needed since the range of the recoil atoms is very short. Two methods were investigated. The first was to evaporate a freshly prepared actinium solution on a stainless steel disc. This method proved ineffective possibly because of the thickness of the evaporated residue. The second method involved the electrodeposition of the actinium onto platinum. This method proved successful and was used throughout this study.

This dissertation will show that the electrodeposition of ^{225}Ac onto platinum will provide a suitable source of recoil atoms and that the electrostatic collection of recoil atoms of ^{221}Fr from the decay of ^{225}Ac will produce ^{213}Bi in high enough yield to be an effective and efficient means of separation and purification, with very little waste production. An equation is also introduced to calculate the activity of ^{221}Fr on the recoil collector.

B. Importance to Nuclear Medicine

Radioisotopes and radioisotope generators have been used extensively in nuclear medicine for the treatment of cancer. [3, 4, 5] The alpha-emitting isotopes are especially important due to the alpha particles' short range and high specific ionization. The alpha particles have energies ranging from 4 – 8 MeV and deposit their energy in a very short distance. The range of an 8 MeV alpha particle is ~ 100 μm in water or about 10 cell diameters. This makes alpha emitters well suited for

destroying tumors and cancer cells without destroying the surrounding tissue. [6] The alpha particle energy, however, is inversely related to its half-life. Therefore, the higher the alpha particle energy the shorter the half-life. This is a major drawback of alpha emitters for use in nuclear medicine, but one that can be overcome with the use of radioisotope generators.

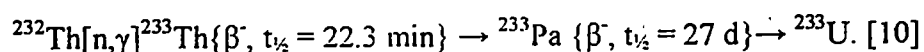
A radioisotope generator or "cow" usually consists of a glass or plastic column containing a cation- or anion-exchange resin. The longer-lived parent isotope is added to the column where it undergoes decay producing the shorter-lived daughter isotopes. The daughter products are then eluted from the column in a way as not to elute the parent isotope. After a period of time, which depends on the daughter half-life, the daughter isotope reaches a maximum activity equal to the activity of the parent isotope and can be eluted or "milked" again. This process is then repeated until the parent isotope has decayed to the point where the amount of daughter produced is no longer useful. At this point, the generator can be either regenerated or disposed as radioactive waste.

As more alpha-emitting isotopes are identified for use in radioimmunotherapy, and radioisotope generators become more prevalent in nuclear medicine to produce these high energy but short half-life isotopes, new and better methods are needed to quickly separate and purify them.

One isotope that has particular promise in fighting cancer is the isotope ^{213}Bi . [7,8,9] Bismuth-213, with a half-life of 45 minutes, is descended from the longer-lived isotope, the ten-day half-life, ^{225}Ac . Actinium-225, in turn, is a member of the Neptunium Series.

PRODUCTION AND DECAY SCHEMATICS OF THE NEPTUNIUM SERIES

The Neptunium ($4n + 1$) Series, see Figure 1 (p 6) and Figure 2 (p 7), unlike the other three naturally occurring series, is extinct because the parent, ^{233}U , has a half-life ($1.592\text{E}+05$ years) which is short compared to the age of the Earth ($4.5\text{E}+09$ years). However, ^{233}U was produced at Oak Ridge National Laboratory (ORNL) in the 1960's and 1970's as part of the molten salt breeder reactor program. Several hundred kilograms of ^{233}U were made by the neutron irradiation of ^{232}Th , by the following reaction:



The ^{233}U is currently in long-term storage and is the only source of high purity ^{229}Th . [7] Thorium-229 (7340 years) is produced by the alpha decay of ^{233}U at a rate of $4.28 \text{ mg (0.91 mCi) kg}^{-1}\text{yr}^{-1}$ and can be extracted and purified by a number of ways. [11] A thorium "cow" is made from the purified thorium, and its daughters, ^{225}Ra (14.9 days) and ^{225}Ac (10 days), after an ingrowth period of ~ 45 days, can be further separated by elution from the anion exchange column with 7.5 N HNO_3 . [10] The ^{225}Ac then alpha decays through a series of short-lived radionuclides: ^{221}Fr (4.9 minutes) to ^{217}At (32.3 milliseconds) to ^{213}Bi (45.59 minutes). This dissertation will focus on the three longer-lived species, ^{225}Ac , ^{221}Fr , and ^{213}Bi .

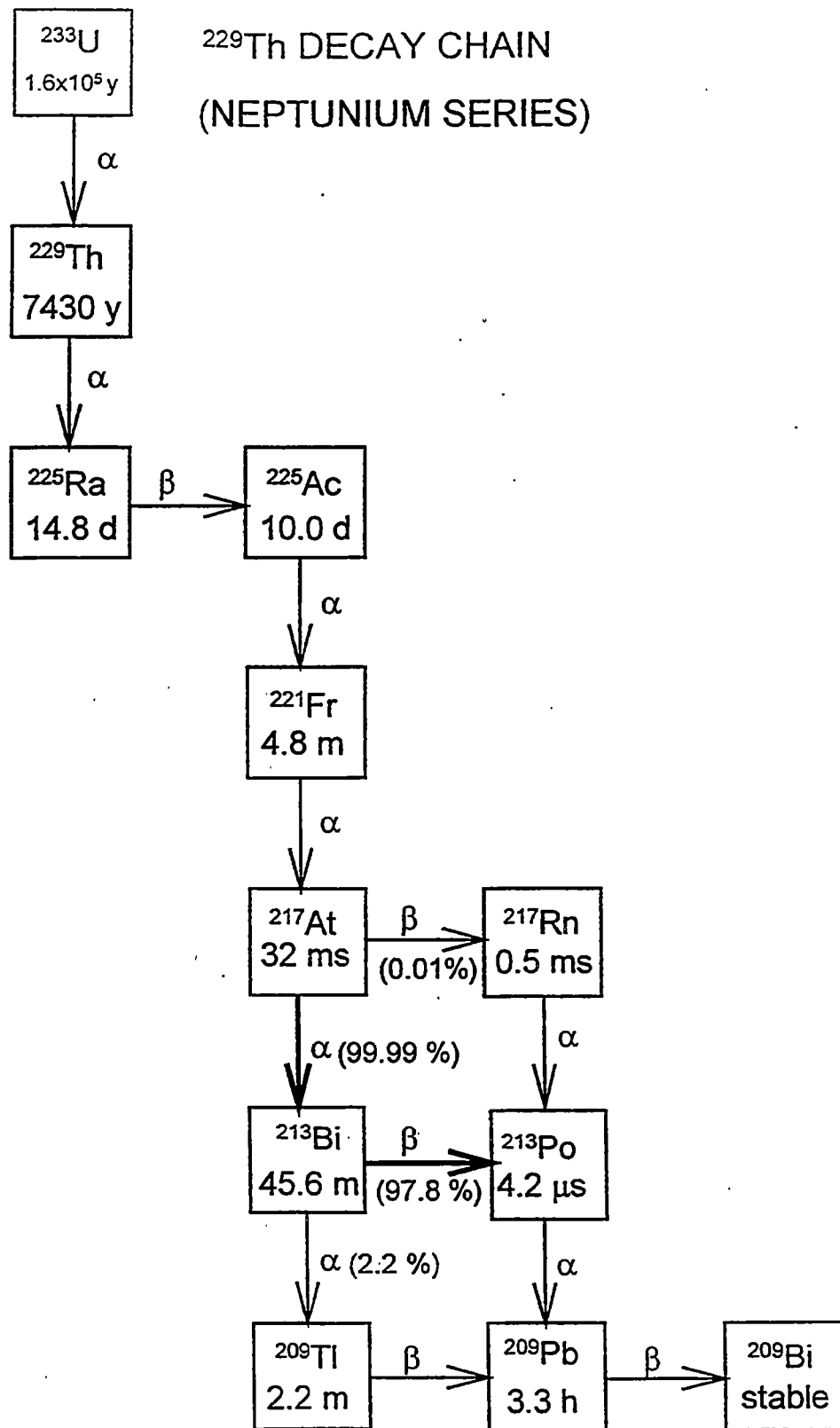


Figure 1. The Neptunium ($4n+1$) Series. [8]

Nuclide	Element name	Half-life	Major radiation energies (MeV) and intensities†		
			α	β	γ
$^{241}_{94}\text{Pu}$	Plutonium	13.2y	4.85 (0.0003%) 4.90 (0.0019%)	0.021 (-100%)	0.145 (0.0016%)
$^{241}_{95}\text{Am}$	Americium	458y	5.44 (13%) 5.49 (85%)	---	0.060 (36%) 0.101c± (0.04%)
$^{237}_{92}\text{U}$	Uranium	6.75d	---	0.248 (96%)	0.060 (36%) 0.208 (23%)
$^{237}_{93}\text{Np}$	Neptunium	2.14×10^6 y	4.65c (12%) 4.78c (75%)	---	0.030 (14%) 0.086 (14%) 0.145 (1%)
$^{233}_{91}\text{Pa}$	Protactinium	27.0d	---	0.145 (37%) 0.257 (58%) 0.568 (5%)	0.31c (44%)
$^{233}_{92}\text{U}$	Uranium	1.62×10^5 y	4.78 (15%) 4.82 (83%)	---	0.042 (?) 0.097 (?)
$^{229}_{90}\text{Th}$	Thorium	7340y	4.84 (58%) 4.90 (11%) 5.05 (7%)	---	0.137c (-3%) 0.20c (-10%)
$^{226}_{88}\text{Ra}$	Radium	14.8d	---	0.32 (100%)	0.040 (33%)
$^{226}_{89}\text{Ac}$	Actinium	10.0d	5.73c (10%) 5.79 (28%) 5.83 (54%)	---	0.099 (?) 0.150 (?) 0.187 (?)
$^{221}_{87}\text{Fr}$	Francium	4.8m	6.12 (15%) 6.34 (82%)	---	0.218 (14%)
$^{217}_{85}\text{At}$	Astatine	0.032s	7.07 (-100%)	---	---
$^{213}_{83}\text{Bi}$	Bismuth	47m	5.87 (-2.2%)	1.39 (-97.8%)	0.437 (?)
$^{213}_{84}\text{Po}$	Polonium	4.2 μ s	8.38 (-100%)	---	---
$^{209}_{81}\text{Tl}$	Thallium	2.2m	---	1.99 (100%)	0.12 (50%) 0.45 (100%) 1.56 (100%)
$^{209}_{82}\text{Pb}$	Lead	3.30h	---	0.637 (100%)	---
$^{209}_{83}\text{Bi}$	Bismuth	Stable ($>2 \times 10^{18}$ y)	---	---	---

*This expression describes the mass number of any member in this series, where n is an integer.

Example: $^{229}_{90}\text{Th}$ ($4n + 1$)..... $4(57) + 1 = 229$

The $(4n + 1)$ series is included here for completion. It is not found as a naturally-occurring series.

†Intensities refer to percentage of disintegrations of the nuclide itself, not to original parent of series.

‡Complex energy peak which would be incompletely resolved by instruments of moderately low resolving power such as scintillators.

Data taken from: Table of Isotopes and USNRDL-TR-802.

Figure 2. Decay Energies of the Neptunium ($4n + 1$) Series [9].

The major gamma decay characteristics of these three radionuclides are given in Table II (p 9). The energies given are the three that were used to quantify the isotopes in this study. A gamma spectrum of the ^{225}Ac source in equilibrium with its daughters is shown in Figure 5 (p 29). All three energies are prominently displayed along with a peak at 117.2 keV that belongs to ^{209}Tl , a daughter of ^{213}Bi . Occasionally, a trace of ^{225}Ra was also present at 40.3 keV.

Gamma spectroscopy was performed on a 50-cm³ high purity germanium (HPGe) detector with a beryllium window. The EG&G reverse electrode Gamma-X detector had an operating voltage of -3500 volts. It was cooled to liquid nitrogen temperature and had a resolution of 1.8 keV at the 1.332 MeV ^{60}Co photopeak. It had a 20% efficiency (relative to a 3 x 3 NaI(Tl) detector), and shelf efficiencies were determined by counting a NIST traceable point source (SRM 4275C-78) of $^{154,155}\text{Eu}/^{125}\text{Sb}$ at different distances (shelves) from the detector in a 2.5 inch thick lead tomb. The shelf efficiencies used in this study are given in Table III (p 10), and the efficiency curves are given as Figure 3 (p 11s). The HPGe detector had a built-in field effect transistor (FET) pre-amplifier to help reduce noise. This was connected to an amplifier, which was connected to an internal Canberra Accuspec PC based analog-to-digital converter (ADC), which displayed the spectrum using 4096 channels. Regions-of-interest (ROIs) were created for each of the peaks of interest and the counts and count time were entered into an Excel© spreadsheet for final analysis. Measurements were made on the initial solution before and after electrodeposition, the cathode after electrodeposition of the actinium, and the atom recoil collector (ARC) after collection.

TABLE II.

MAJOR GAMMA CHARACTERISTICS OF ^{225}Ac , ^{221}Fr , AND ^{213}Bi . [13]

Isotope	Half-life	Energy (keV)	% Photon Abundance
^{225}Ac	10 days	187.99	0.465
^{221}Fr	4.9 minutes	217.98	11.58
^{213}Bi	45.59 minutes	440.34	26.1

TABLE III.

SHELF EFFICIENCIES

Gamma Detector Efficiency Curves at Selected Distances from Detector in Room 311, Building 4501, ORNL 1/25/99									
Energy (keV)	I _g %	30 cm	25 cm	20 cm	15 cm	10 cm	5 cm	2 cm	1 cm
188	0.47	9.990E-04	1.392E-03	2.006E-03	3.277E-03	6.486E-03	1.862E-02	4.827E-02	1.931E-01
217.6	11.58	8.970E-04	1.248E-03	1.880E-03	3.072E-03	6.078E-03	1.738E-02	4.500E-02	1.800E-01
440	26.1	4.510E-04	6.210E-04	9.326E-04	1.532E-03	3.016E-03	8.105E-03	2.044E-02	8.176E-02

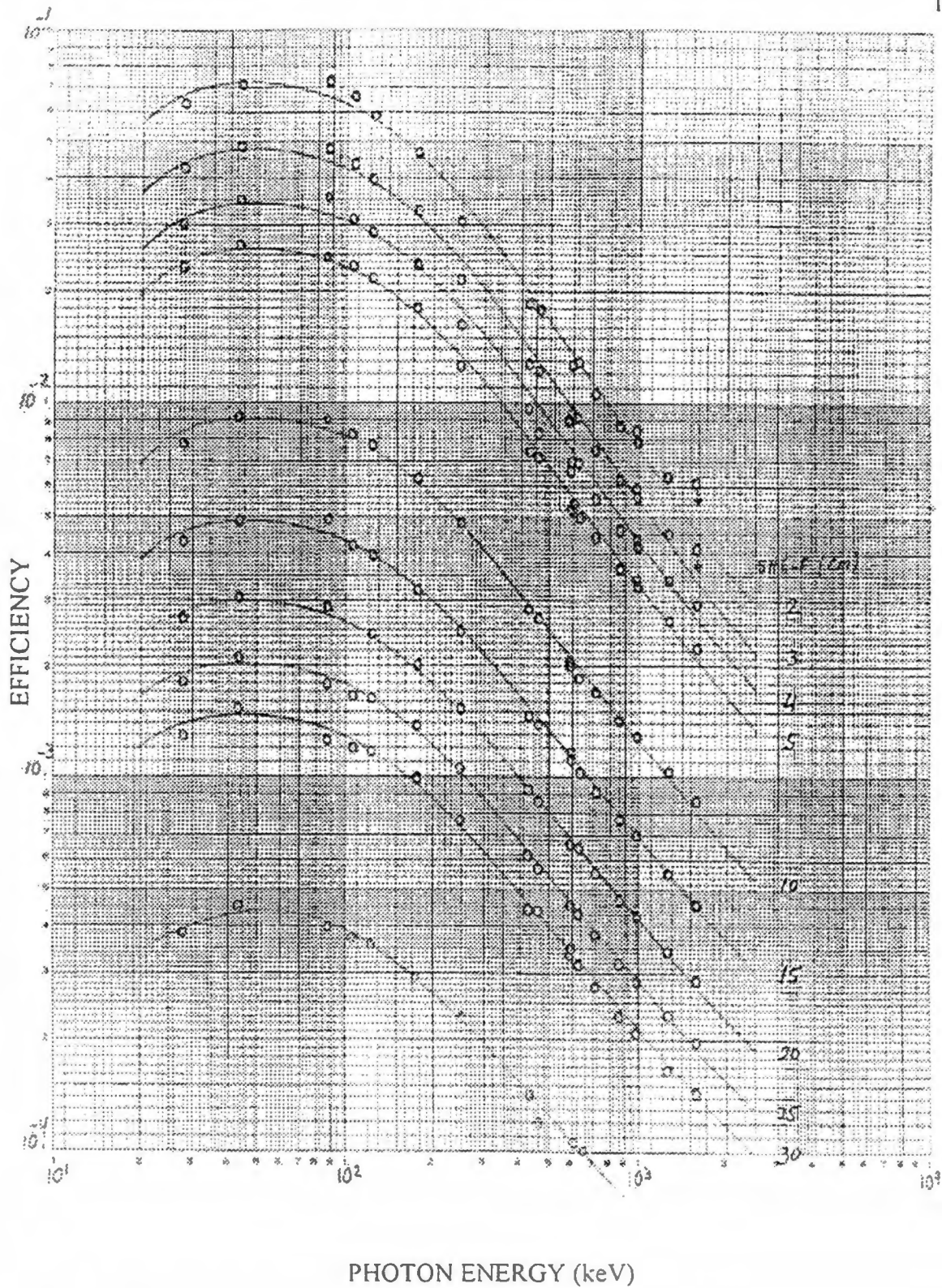


Figure 3. Efficiency curves for Gamma-X detector.

Using the following formulas, corrections were made to relate the measured activities on the atom recoil collector back to the starting activities.

C.F.1 = $1/(1 - e^{-\lambda t})$ The correction factor for decay of the ^{221}Fr and ^{213}Bi during the recoil collection.

C.F.2 = $1/(e^{-\lambda t})$ The correction factor for decay of the ^{221}Fr and ^{213}Bi during the transfer time between the end of recoil collection and the beginning of the count time.

C.F.3 = $\lambda t/(1 - e^{-\lambda t})$ The correction factor for decay of the ^{221}Fr and ^{213}Bi during the count time.

These correction factors were multiplied by the measured activities of ^{221}Fr and ^{213}Bi prior to calculating the yield of the recoil process. The yield of the recoil process was the corrected measured activities divided by the starting activities of the ^{221}Fr and ^{213}Bi on the cathode.

CHAPTER III

HISTORICAL INFORMATION

This dissertation was a feasibility study to show that the collection of recoil atoms from a decaying ^{225}Ac source would be practicable for the production of ^{221}Fr and ^{213}Bi atoms. The recoil technique was decided upon because it could theoretically produce pure ^{213}Bi with little need of radiochemical separations, has very little waste production, and can be scaled-up to 100 mCi (a useful clinical generator).

The radioactive recoil technique was discovered by Otto Hahn in 1909. [10] The method is based on the recoil of the daughter nucleus after the emission of an alpha particle by the parent nucleus as required by the conservation of momentum. An equation for the recoil energy of the daughter nucleus can be derived from the Law of Conservation of Energy and the Law of Conservation of Momentum in terms of the alpha decay energy, E_{α} :

$$E_R = (M_{\alpha}/M_R) E_{\alpha},$$

where M_{α} is the mass of an alpha particle and M_R is the mass of the recoil (daughter) nucleus. This equation can be rewritten approximating the masses with the mass numbers of the parent nucleus, A , and using the mass number of helium for the alpha particle to give:

$$E_R = 4E_{\alpha}/(A - 4),$$

where $A - 4$ would be the mass number of the daughter nucleus. Using this equation, the recoil energies of the isotopes of interest are presented in Table IV (p 14).

TABLE IV.
RECOIL ENERGIES OF THE ISOTOPES

Isotope		Mass Number, A of Parent	Alpha Energy, E_α (MeV)	Recoil Energy, E_R^a (MeV)
Parent	Daughter			
^{225}Ac	^{221}Fr	225	5.83	0.10
^{221}Fr	^{217}At	221	6.34	0.12
^{217}At	^{213}Bi	217	5.87	0.11

$$^a E_R = 4E_\alpha / (A - 4)$$

The kinetic energy of the recoil atoms are all about 0.1 MeV, which corresponds to a velocity of $\sim 3.06 \times 10^5$ m/s ($KE = \frac{1}{2}mv^2$). This is a sufficient velocity to strip the outer orbital electrons, because the moving atoms (ions) become stripped of all orbital electrons whose orbital velocity is less than the velocity of the atom (ion). [11,14] As the atom (ion) slows down, it begins to pick up electrons. Therefore, its charge is greater just after the recoil than it is at the end of its range. At velocities greater than 2.0×10^6 m/s the ions major loss of energy is by ionization and excitation of atoms in the surrounding medium. [14] At velocities below 2.0×10^6 m/s, the main energy loss is by elastic scattering. [14] In this region, the ratio of the mass of the recoil atom M_1 to the mass of the stopping medium M_2 determines the behavior of the ion. If the ratio M_1/M_2 is large, then the average energy loss per collision will be small and the ions will travel in nearly straight lines. [14] If the ratio of the masses is unity or less, then the paths will be far from straight. At a ratio of one, the ion may lose a large fraction of its energy in a single collision, therefore, its range is proportional to its energy. [14] For alpha decay, the ratio M_1/M_2 is less than one and the recoil daughter nucleus will lose most of its energy by elastic scattering during a random walk. However, the electrostatic field tends to straighten the path in the direction of the field because the multiple positive charges are attracted to the negatively charged plate. The electrostatic field also imparts an additional 5 keV of energy per charge to the ion (see Table 1, p 2), thus extending its range.

Separations based on the recoil process, with subsequent collection of the positively charged ions on a negatively charged plate, has been used in the past to separate and collect charged particles. As early as 1899, Ernest Rutherford was

collecting charged particles from thorium oxide between electrically charged plates. [15] More recently, this process has been used to collect the short-lived actinium isotopes {222 (5.5 s), 223 (2.2 min), and 224 (2.9 h)} [11] and to elucidate artificial short-lived decay chains collateral to the natural decay chains [16,17]. Meinke et al. used an electric field between two plates where the recoil atoms were collected on the negatively charged plate. They reported a yield for this type of recoil collection of ~10 percent. They also reported that yields of 50 percent can be obtained in vacuum without the need of an electric field. [16]

Ghiorso et al. have applied a double recoil technique to the discovery of isotopes of the newer elements nobelium [18, 19] and lawrencium [20]. These involved very sophisticated apparatus with high vacuums, intense ion beams to induce nuclear reactions, and helium carrier gas to move the recoiled atoms to a thin copper conveyor tape, which then moved the collected recoil atoms to a series of solid-state surface-barrier detectors. [20]

Recoil collections by gas entrainment have also been used to study accelerator-produced short-lived alpha emitters. [21,22] MacFarlane and Griffioen reported an overall collection efficiency (defined as the number of recoils collected to the number atoms ejected from the target) of 0.6. [21]

More recent attempts involve capturing recoils from an orthotropic source [23] in a vapor cell magneto-optical trap where the atoms are thermalized in an oven to produce an atomic beam of ^{221}Fr atoms [24]. This arrangement produced a flux of $3.8\text{E}+04$ atoms per second of ^{221}Fr with a yield of about 2%. [24]

To summarize, most efforts to use recoil techniques to separate atoms involved sophisticated apparatus and high vacuums to get low to moderate yields. This research will show that high yields can be obtained, in air, with an electrostatic field and with very simple apparatus.

CHAPTER IV

SOURCE PREPARATION BY EVAPORATION

Much time was given to source preparation. Initially, the source consisted of a glass or stainless steel disc on which about 150 μL of ^{225}Ac in 0.1 N HNO_3 acid solution was evaporated under a heat lamp, until the residue was dry. Many attempts were made to spread the residue as thinly as possible. In addition, different voltages were tried to "pull" the recoil atoms through the residue, without success. Mica was used as a dielectric to increase the capacitance of the plates, but improvements were minimal. Even collection in a vacuum was unsuccessful. The process of evaporation apparently left a residue too thick for the recoiling atoms to escape, although sources prepared by evaporation were well suited for gamma spectroscopy. [25]

The impurities, as assayed by the manufacturer, in the ultrapure HNO_3 acid used for the actinium extraction are listed in Table V (p 19). [26] The numbers of atoms of all the impurities cover fewer than three percent of the area of the disc if the atoms were arranged in a monolayer across the surface of the disc. If a hundred microcuries (μCi) of ^{225}Ac were a part of the solution evaporated and were allowed to reach equilibrium with ^{221}Fr and ^{213}Bi , then the number of atoms arranged in a monolayer on the surface of the disc would still cover less than three percent of the disc. However, the residue was not evenly distributed, as evidenced by the appearance of a white residue on the disc.

TABLE V.
PARAMETERS AND CONCENTRATIONS OF IMPURITIES IN ULTRAPURE NITRIC ACID [26]

Element	Atomic Radius cm	Area cm ² /atom	Conc. ppb	Atoms	Total Area of Atoms cm ²	% Area of Disc
Cr	1.30E-08	5.31E-16	5	7.211E+13	3.83E-02	1.22%
Fe	1.26E-08	4.99E-16	2	2.685E+13	1.34E-02	0.43%
Na	1.90E-08	1.13E-15	1	3.262E+13	3.70E-02	1.18%
				SUM =	8.87E-02	2.82%
Ac-225	1.88E-08	1.11E-15	uCi	4.544E+12	5.05E-03	0.16%
Fr-221	2.70E-08	2.29E-15	100	1.547E+09	3.54E-06	0.000113%
Bi-213	1.70E-08	9.08E-16	100	1.438E+10	1.31E-05	0.000416%
				SUM =	5.06E-03	0.16%
TOTAL % =						2.98%

The range of recoiled ^{221}Fr in different matrices was calculated using the expression of Bohr for ions with an initial velocity below $2.0\text{E}+08$ cm/s. (The 0.1 MeV recoil energy of the ^{221}Fr daughter translates into a recoil velocity of $3.06\text{E}+07$ cm/s). The Bohr equation is:

$$R_0 = \Omega \times E_R \times (M_2(M_1+M_2)/M_1) \times (Z_1^{2/3} + Z_2^{2/3})^{1/2} / (Z_1 \times Z_2)$$

where E_R is the recoil energy of an ion of mass M_1 and atomic number Z_1 , moving in a stopping medium of mass M_2 and atomic number Z_2 . [22] The proportionality constant Ω has a value of 600. [22] The ranges calculated for recoiled ^{221}Fr in different matrices are given in Table VI (p 21). From these data, the range is on the order of a few hundred angstroms (\AA) or tenths of a nanometer (nm), clearly less than the thickness of any visible residue. These values are in agreement (same order of magnitude) with that calculated by Gould (300\AA). [2] Indeed, if 100 μCi of ^{225}Ac were spread in a monolayer over a disc of 4.5 cm^2 , the resulting thickness would be only 0.0038\AA , which is less than its atomic radius of 1.88\AA and its ionic radius of 1.11\AA . This implies that there is plenty of room for a monolayer of ^{225}Ac with room to spare. A reverse calculation shows that 45.5 mCi of ^{225}Ac would be required to cover completely the 4.5 cm^2 area one atom thick.

It had been hoped that the evaporation technique would be sufficient because of the simplicity of the technique and the minimal equipment needed. However, it was soon obvious that the evaporation technique was ineffective and that another technique was needed. The electrodeposition of actinium onto a platinum electrode was then investigated.

TABLE VI.
CALCULATED RANGES OF RECOILED ^{221}Fr IN DIFFERENT MATRICES

Element	M_1^*	M_2	Z_1^*	Z_2	ρ (g/cm^3)	R_0 (mg/cm^2)	R_0 (cm)	R_0 (\AA)
Na	221	22.9898	87	11	0.97	7.89	8.13E-06	813
Cr	221	51.9961	87	24	7.19	9.76	1.36E-06	136
Fe	221	55.847	87	26	7.874	9.89	1.26E-06	126
Cu	221	63.546	87	29	8.96	10.49	1.17E-06	117
Pt	221	195.08	87	78	21.45	19.99	9.32E-07	93
Ac	221	225	87	89	10.07	22.13	2.20E-06	220
Air	221	29.089	87	80	0.001226	1.75	1.43E-03	14 μm

* M_1 and Z_1 refer to ^{221}Fr

CHAPTER V

A SUMMARY OF ACTINIUM SOLUTION CHEMISTRY

Actinium, element 89, is the first member of the actinide series or actinides. It is the second rarest of the naturally occurring elements and has 31 isotopes. [27] All the isotopes of actinium are radioactive. The two most common isotopes are ^{227}Ac ($t_{1/2} = 21.773$ years) of the Actinium Series ($4n + 3$) and ^{228}Ac ($t_{1/2} = 6.13$ hours) of the Thorium Series ($4n$). [28] Only the Uranium Series ($4n + 2$) does not have an actinium isotope in its decay chain. It is not found in nature by itself, but can be separated from uranium and thorium ores. The extinct Neptunium Series ($4n + 1$) contains the second longest-lived actinium isotope, ^{225}Ac ($t_{1/2} = 10$ days).

Based on the position of actinium in the Periodic Table as a member of a d-transition series with a $6d^1 7s^2$ electronic structure in its ground state, the +3 oxidation state would seem to be the only valence of any practical importance. This has been confirmed by redox potential measurements in which the standard potential, E^0 , for the $\text{Ac}^{\text{III}}|\text{Ac}^0$ reduction, was measured to be -2.13 volts. [10] There was little to no evidence to support the existence of a +2 oxidation state. [10] Therefore, the most chemically stable state of the element actinium in solution is the +3 oxidation state. Actinium is found in this state over the entire water stability range. See Pourbaix Diagram in Figure 4 (p 23).

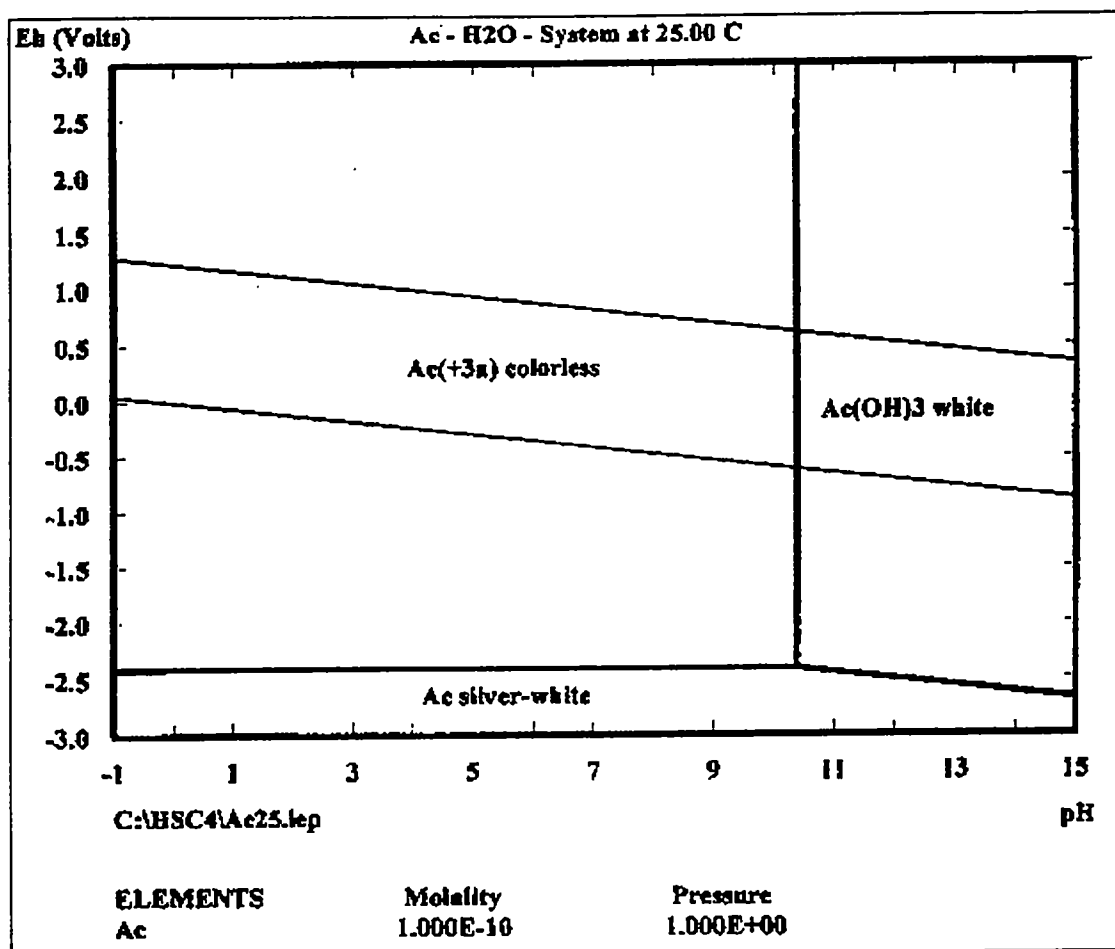


Figure 4. Pourbaix diagram for actinium.

This trivalent element is in Group IIIB of the Periodic Table, which makes it analogous to lanthanum, and indeed it shows a strong chemical similarity to lanthanum. [10] Actinium ($[\text{Rn}]5d^16s^2$) is clearly then a homologue of lanthanum ($[\text{Xe}]6d^17s^2$) by virtue of both its chemical behavior and its electronic structure. Its compounds are all isomorphous with the corresponding lanthanum compounds and its solutions are colorless. [10] With an ionic radius of 1.11 Å, actinium is the largest tripositive cation known. [10] It forms radiocolloids at a pH of 6 or higher and will adsorb onto glass at a pH of 5. [10] It is also important to use a freshly prepared solution. Mueller has shown that an aged $\text{Ac}(\text{NO}_3)_3$ solution contains up to 99% of the element in a colloidal state and that to transform it back to its ionic form requires repeated boiling with nitric acid and evaporation to near dryness. [28]

Actinium undergoes hydrolysis at a pH of 5 to 6 forming $\text{Ac}(\text{OH})^{2+}$. [10] At a pH of 8, nearly 100% of the actinium is in the form $\text{Ac}(\text{OH})^{2+}$ and $\text{Ac}(\text{OH})_2^+$, although the hydrolysis constants have yet to be determined. [10] Therefore, it is very important for the pH of the solution to be ≈ 2 to keep the trivalent form, Ac^{+3} , the predominant form in solution. Actinium also undergoes complex formation with chloride and nitrate ions. The chloride forms have been identified as AcCl^{2+} , AcCl_2^+ , and AcCl_3^0 . Their formation constants are given in Table VII (p 25). There is also evidence of an anionic complex, AcCl_4^- . Nitrate forms the complexes: $\text{Ac}(\text{NO}_3)^{2+}$ and $\text{Ac}(\text{NO}_3)_2^+$. The nitrate complexes are remarkable in that they form only in the presence of high concentrations of nitrate salts, especially LiNO_3 , but not in concentrated nitric acid having the same nitrate anion concentration. [10] The formation constants for these nitrate complexes are also found in Table VII (p 25).

TABLE VII

Complex Formation Constants of Actinium with Chloride and Nitrate [7]

Reaction	Method	Formation Constant
$\text{Ac}^{3+} + \text{Cl}^- \rightleftharpoons \text{AcCl}^{2+}$	1	0.91
	2	0.8
$\text{Ac}^{3+} + 2\text{Cl}_2^- \rightleftharpoons \text{AcCl}_2^+$	1	0.091
	2	0.24
$\text{Ac}^{3+} + 3\text{Cl}^- \rightleftharpoons \text{AcCl}_3^0$	1	0.055
$\text{Ac}^{3+} + \text{NO}_3^- \rightleftharpoons \text{Ac}(\text{NO}_3)^{2+}$	2	1.31
$\text{Ac}^{3+} + 2\text{NO}_3^- \rightleftharpoons \text{Ac}(\text{NO}_3)_2^+$	2	1.02

Method 1: dis/TTA; 4 M NaClO₄; 25°C

Method 2: dis/DNNS; 1M HClO₄; 27°C

dis: distribution between two liquid phases

TTA: 2-thenoyltrifluoroacetone

DNNS: dinonylnaphthalene-sulfonic acid

CHAPTER VI

THE ELECTRODEPOSITION OF ACTINIUM

Because of the very negative standard electrode potential ($E^0 = -2.13$ V), actinium metal should not electrochemically deposit on the cathode from an aqueous solution.[10] Whatever the chemical form of the actinium, it does electrodeposit, and several papers have been published with procedures to do so. [10,29,30] Possible explanations include adsorption onto the cathode material or onto a carrier present in the solution followed by deposition of the carrier with the actinium at the cathode. [7]

References 10 and 29 report the use of a saturated urea oxalate solution from which carrier-free ^{227}Ac is electrodeposited with a current density of 20 to 80 mA/cm² onto a nickel foil cathode (the anode consisted of a platinum wire). [10,29] These methods gave yields of 90% - 95% after two hours of deposition. [10,29] These two methods were decided against because of the concern that the oxalate would also coat the surface and prevent the recoil daughter atoms from escaping. A third method [31] did not have this drawback and gave yields of nearly 100% after only one hour of deposition time.

This third method consisted of electrodepositing carrier-free ^{227}Ac from a nitric acid solution of pH = 2. [30] The electrodes consisted of a platinum disc for the cathode and a spiral platinum wire for the anode. After the electrolysis, ammonium hydroxide was added to make the solution alkaline before turning off the current. A current density of 200 mA/cm² for one hour gave a yield of ~100%. [30] Because this approach took less time and the ^{225}Ac was already in a nitric acid solution, this method, with some modifications, was used.

The method used here consisted of electrodepositing ^{225}Ac from a nitric acid solution of pH ~ 2 . The electrochemical cell was a 20-mL glass scintillation vial. The cathode was a 1.5 cm x 1.5 cm platinum square (active area of 4.5 cm²) spot welded to a 5 cm platinum wire. The anode was also a 5 cm platinum wire. The electrodes were prepared by washing with concentrated nitric acid, rinsing with Millipore (18 M Ω) deionized (DI) water, and blotting dry. The pH of the solution was not adjusted to a pH of 2, but the source preparation was designed to give a solution of pH ~ 2 when the carrier-free ^{225}Ac was diluted to 15 mL with 0.01 N nitric acid. The calculated pH, based on the nitric acid concentration only, was 1.96, and the measured pH, which also included ^{225}Ac , was measured with pH paper to be 1.6. The electrodes were placed ~ 0.5 cm apart with the cathode attached to the negative terminal of a Hewlett Packard E3610A DC power supply and the anode to the positive terminal. A potential difference of 8 volts was then applied between the electrodes. The electrodeposition was allowed to continue for one hour while the solution was stirred magnetically. At the end of the electrodeposition period, the cathode was removed from the solution prior to turning off the voltage. No ammonium hydroxide was added. The 20 mL vial containing the ^{225}Ac solution, was analyzed for ^{225}Ac before and after the electrodeposition, to determine the amount of ^{225}Ac deposited. The cathode was also counted to determine the source activity. The electrodeposition was also run at 12 volts and at one-cm distance between the electrodes, with comparable results. The detailed step-by-step procedures for the source solution preparation and the electrodeposition are given in Appendix I (p 82) and Appendix II (p 83), respectively.

The main difference between our method and that of Iyer et al. [29] was the current density. Whereas the method in Reference 25 specified a current density of 150 – 250 mA/cm² for one hour at pH = 2, this work gave the same yields (~98%) for the same duration but with a much lower current density of ~ 13 to 22 mA/cm² in our case. It is not known at this time why such a large difference in current density would give the same yields for the same deposition time.

Figures 5 (p 29) and 6 (p 30) are spectra of the source solution before and after the electrodeposition, respectively. The top part of the spectra is an expanded view of the lower part of the spectrum. The spectra show clearly the removal of ²²⁵Ac by the absence of the ²²⁵Ac peak at 188 keV (location of the cursor) in Figure 6 (p 30).

Figure 7 (p 31) shows the decrease of ²²⁵Ac in solution during the electrodeposition, and Figure 8 (p 32) shows the corresponding increase of ²²⁵Ac on the cathode. These data were collected by taking 100 uL aliquots of the solution every 15 minutes during a three-hour electrodeposition period. The aliquots were counted for two minutes. As can be seen from the graphs, 98% to 99% of the actinium was removed from the solution and deposited onto the cathode within 60 minutes. Thereafter, the electrodepositions were carried out for one hour. The data are reported in Table VIII (p 33) and Table IX (p 34) gives the electrode parameters and shows data from a typical electrodeposition. The negative numbers in Table VIII (p 33) for the activities and atoms are the result of negative count rates.

Once the electrodeposition was complete, the daughters were allowed to reestablish equilibrium. The cathode was then counted to get a more accurate measure of ²²⁵Ac on the cathode. This was done because the flat cathode was

20-May-00 19:39:03 SP= MCA1/1 OFF CFS 65536/ALIN CC 374/ 188.277

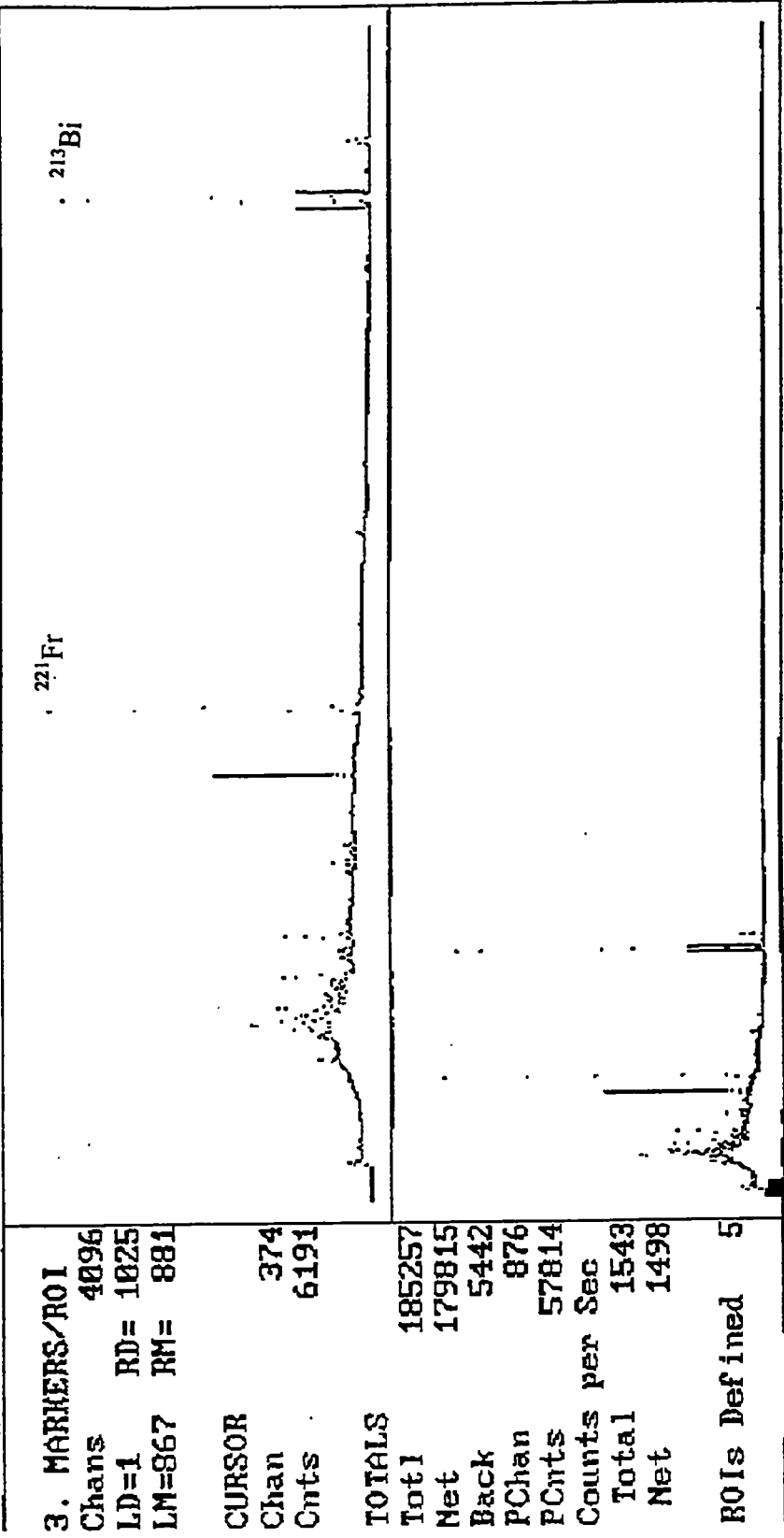


Figure 5. Gamma spectrum of ²²⁵Ac solution prior to electrodeposition showing the presence of ²²⁵Ac at 188 keV.

21-May-88 22:26:13 SP= MCA1/1 OFF CFS 32768/ALIn CC 374/ 188.277

3. MARKERS/ROI
 Chans 4896
 LD=1 RD= 1025
 LM=369 RM= 379

CURSOR
 Chan 374
 Cnts 1093

TOTALS
 Totl 10608
 Net 510
 Back 10090
 PChan 374
 PCnts 1093
 Counts per Sec
 Total 88
 Net 4

ROIs Defined 5

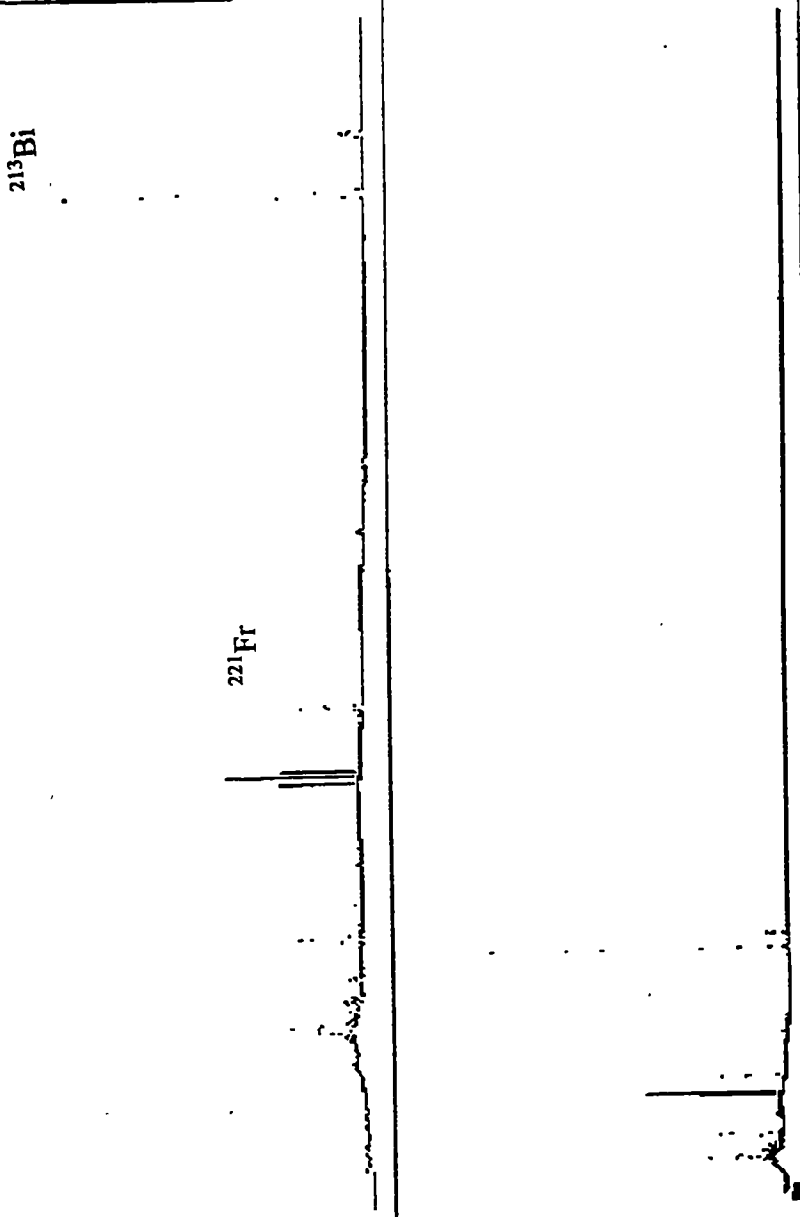


Figure 6. Gamma spectrum of ^{225}Ac solution after electrodeposition showing the absence of ^{225}Ac at 188 keV.

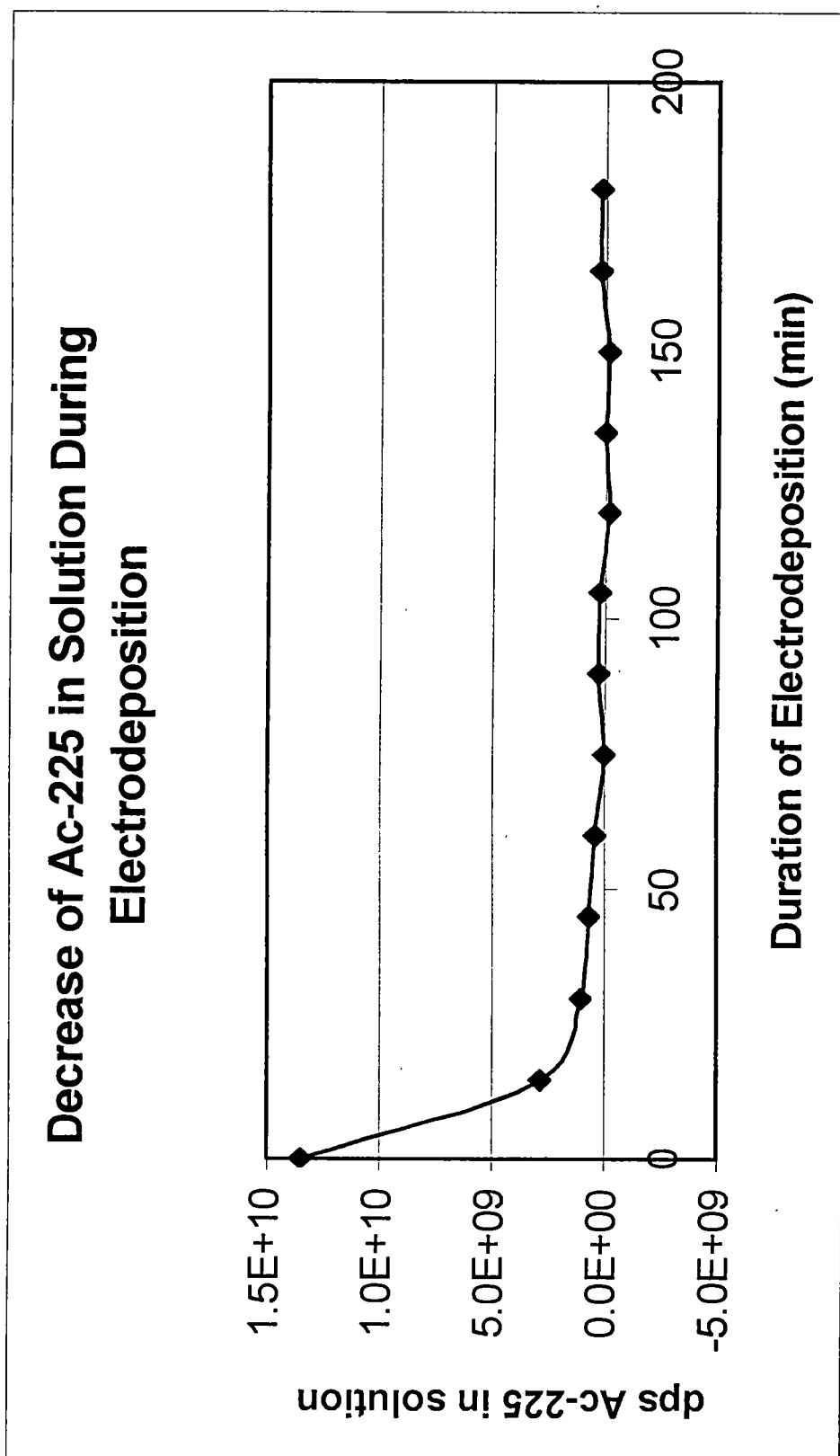


Figure 7. Decrease of ²²⁵Ac in solution during electrodeposition.

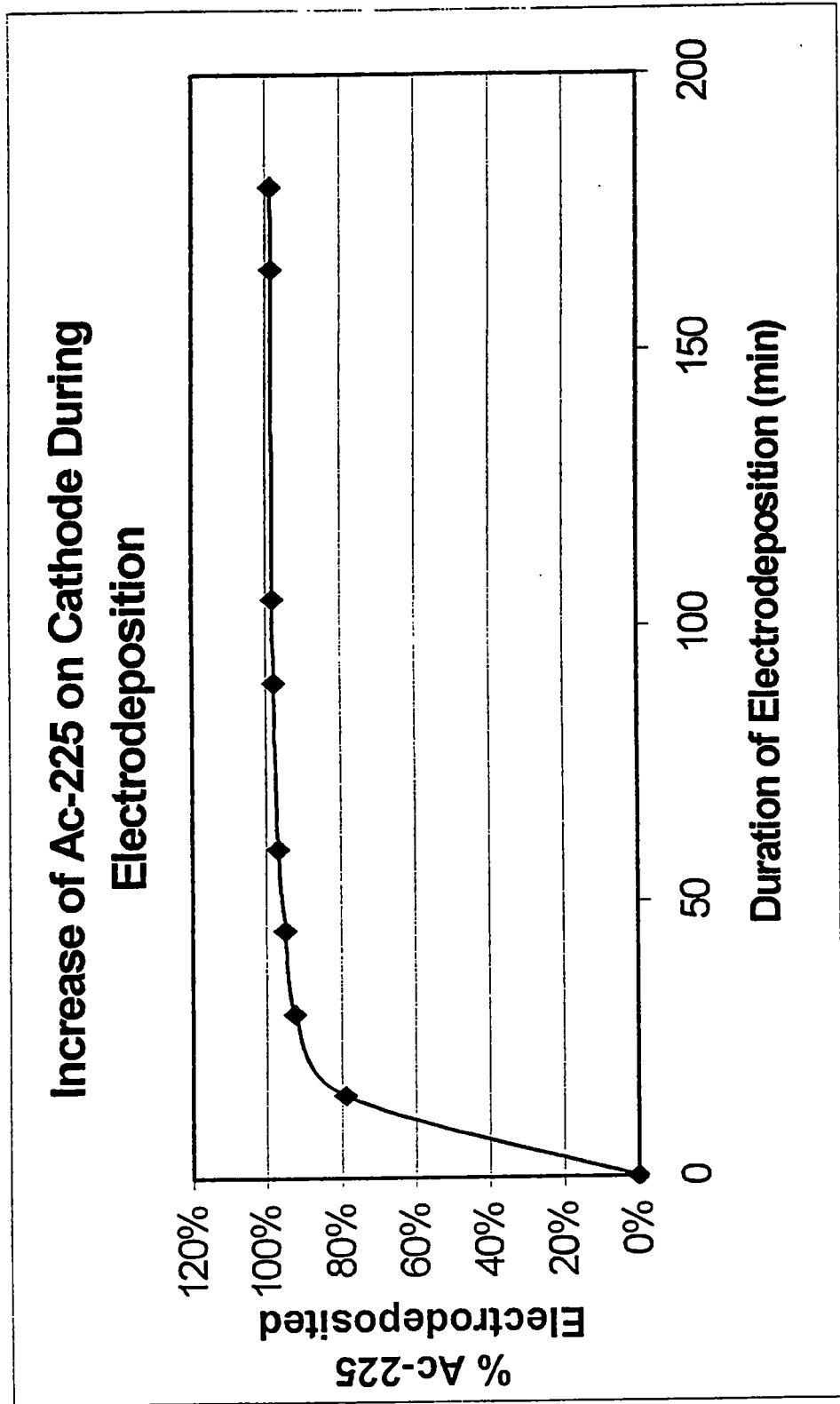


Figure 8. Increase of ²²⁵Ac on cathode during electrodeposition.

TABLE VIII

ACTIVITY OF ²²⁵AC IN SOLUTION AND AFTER ELECTRODEPOSITION AT PROGRESSIVE TIME INTERVALS

t1 (min)	Counts	C.F.1	C.F.2	C.F.3	shelf cm	Efficiency cps/dps	Ac-225 in solution			Ac-225 electroplated			N/N ₀
							dps	uCi	atoms, N	dps	uCi	atoms, N	
0	2955	1.0	1.0	1.0	1	1.93E-01	1.09E+04	2.93E-01	1.35E+10	-----	-----	-----	
15	624	1.0	1.0	1.0	1	1.93E-01	2.29E+03	6.20E-02	2.86E+09	8.56E+03	2.31E-01	1.07E+10	7.89E-01
30	222	1.0	1.0	1.0	1	1.93E-01	8.16E+02	2.20E-02	1.02E+09	1.00E+04	2.71E-01	1.25E+10	9.25E-01
45	149	1.0	1.0	1.0	1	1.93E-01	5.47E+02	1.48E-02	6.82E+08	1.03E+04	2.79E-01	1.28E+10	9.50E-01
60	93	1.0	1.0	1.0	1	1.93E-01	3.42E+02	9.23E-03	4.26E+08	1.05E+04	2.84E-01	1.31E+10	9.69E-01
75	1	1.0	1.0	1.0	1	1.93E-01	3.67E+00	9.93E-05	4.58E+06	1.09E+04	2.93E-01	1.35E+10	1.00E+00
90	63	1.0	1.0	1.0	1	1.93E-01	2.31E+02	6.26E-03	2.89E+08	1.06E+04	2.87E-01	1.32E+10	9.79E-01
105	50	1.0	1.0	1.0	1	1.93E-01	1.84E+02	4.96E-03	2.29E+08	1.07E+04	2.88E-01	1.33E+10	9.83E-01
120	-35	1.0	1.0	1.0	1	1.93E-01	-1.29E+02	-3.48E-03	-1.60E+08	1.10E+04	2.97E-01	1.37E+10	1.01E+00
135	0	1.0	1.0	1.0	1	1.93E-01	0.00E+00	0.00E+00	0.00E+00	1.09E+04	2.93E-01	1.35E+10	1.00E+00
150	-25	1.0	1.0	1.0	1	1.93E-01	-9.18E+01	-2.48E-03	-1.14E+08	1.09E+04	2.96E-01	1.36E+10	1.01E+00
165	48	1.0	1.0	1.0	1	1.93E-01	1.76E+02	4.77E-03	2.20E+08	1.07E+04	2.89E-01	1.33E+10	9.84E-01
180	37	1.0	1.0	1.0	1	1.93E-01	1.36E+02	3.67E-03	1.69E+08	1.07E+04	2.90E-01	1.34E+10	9.87E-01

t1 is the time between voltage on and voltage off

t2 is the time between voltage off and begin counting = 30 sec

t3 is the count time = 300 sec

Used the 188 keV gamma ray to quantitate the ²²⁵Ac

TABLE IX.

ELECTRODE PARAMETERS AND YIELD CALCULATION FOR ELECTRODEPOSITION

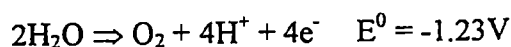
Pt cathode geometry factor	length (cm)	width (cm)	area (cm ²)	Amperage (A)	current density (mA/cm ²)	Voltage (V)	Resistance (ohms)
2	1.5	1.5	4.5	0.06	13.33	12	200.00
t1	t2	t3	Ac-225 Counts before	10 day half-life Counts after	t1	t2	t3
0	0	120	4884	31	C.F.1	180	120
	C.F.2	C.F.3			C.F.1	C.F.2	C.F.3
	1.000	1.000			1.000	1.000	1.000
Source to Detector Distance = 25cm							
Efficiency = 1.39E-03							
cps = 40.70							
uCi = 1.68E+02							
dps = 6.22E+06							
atoms = 7.755E+12							
4.923E+10							
1.67E+02 uCi Ac-225 plated on cathode							
6.18E+06 dps Ac-225 plated on cathode							
7.7055E+12 atoms Ac-225 plated on cathode							
1.2793E-11 moles Ac-225 plated on cathode							
99.37% yield for electrodeposition							
t1 is the time between voltage on and voltage off							
t2 is the time between voltage off and begin counting							
t3 is the count time							

in a geometry similar to that of the copper disc use to collect the recoil atoms as opposed to the vial of solution. Figures 9 (p 36) and 10 (p 37) show the buildup of ^{221}Fr and ^{213}Bi , respectively, on the cathode after the electrodeposition was complete.

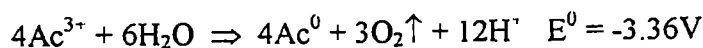
Although the actual species that deposits on the cathode is unknown, for this discussion the electrochemical half-reaction at the cathode is assumed to be:



and the half-reaction at the anode to be:



This gives an overall cell reaction of :



Therefore, the potential difference for the electrodeposition would need to be greater than 3.36V. The Nernst Equation for this reaction is:

$$E = E^0 - (.059/n) * \log ([\text{H}^+]^{12}/[\text{Ac}^{3+}]^4)$$

where $n = 12$. However, the Nernst Equation tends to break down under conditions where the number of atoms in the solution is less than that required to cover the electrodes. We thus move from a thermodynamic to a kinetic description of the electrodeposition process.

The rate of electrodeposition of the actinium on the cathode can be expressed by the following mathematical relationship, first derived by Frederic Joliot in 1930 for the electrodeposition of polonium on gold [27] and later described by Fahland et al. [28], Reischmann et al. [29], and Mirzadeh et al. [30]:

$$dN/dt = \alpha(N_0 - N) - \beta N.$$

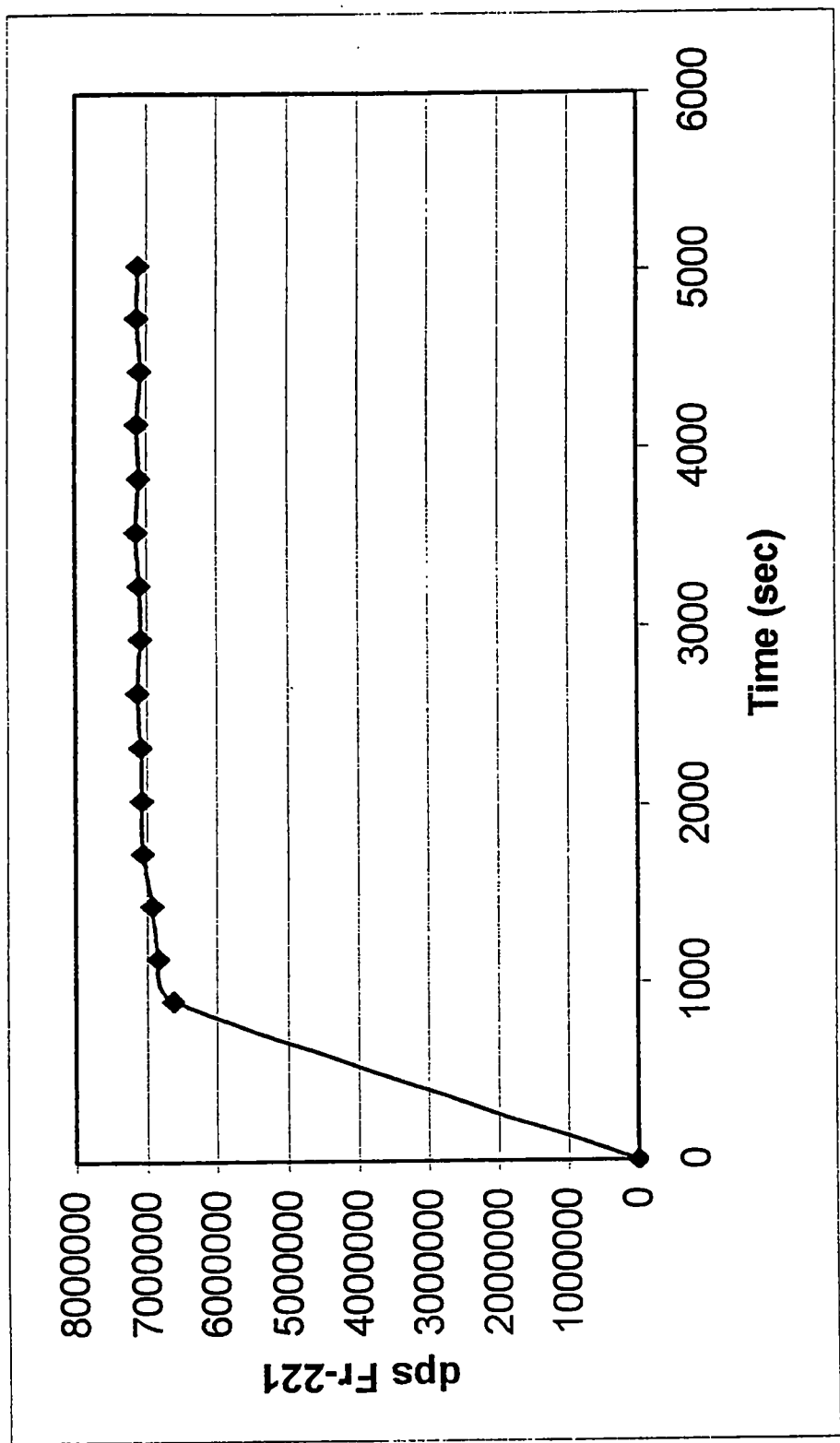


Figure 9. ^{221}Fr activity on cathode after electrodeposition.

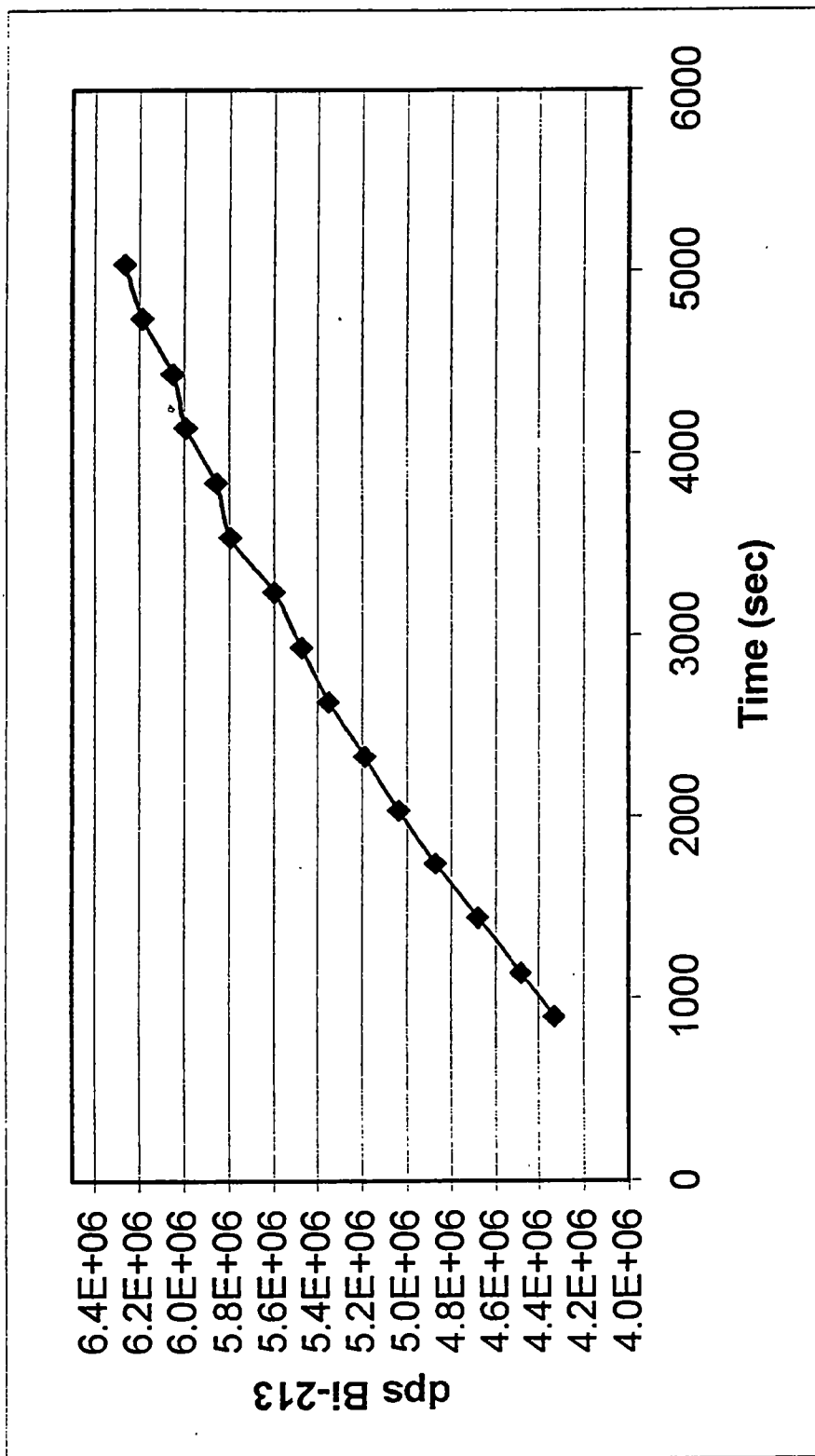


Figure 10. ^{213}Bi ingrowth on cathode after electrodeposition.

In this equation, N represents the number of ^{225}Ac atoms deposited on the cathode during the electrodeposition period, t . N_0 is the initial number of ^{225}Ac atoms in the solution at $t = 0$. Therefore, $N_0 - N$ is the number of ^{225}Ac atoms left in solution at time t . Because α is the deposition velocity constant and β is the dissolution velocity constant, the rate at which the actinium is being deposited on the cathode is proportional to the number of ^{225}Ac atoms in solution available for deposition at any time t , minus the rate at which the actinium is being redissolved off the cathode back into solution. Obviously, for a useful electrodeposition to occur, β needs to be small in comparison to α .

The solution to the differential equation above is:

$$N = \ell * N_0 * e^{-\lambda t} * (1 - e^{\vartheta t}),$$

where ℓ and ϑ are constants to be determined. The constant ℓ is defined as $[\alpha/(\alpha + \beta)]$ and is unitless [34]. ϑ is defined as $(\alpha + \beta)$ and has units of min^{-1} [33]. In this case, the ^{225}Ac half-life ($t_{1/2} = 10$ days) is much longer than the deposition time ($t = 60$ minutes) so the decay correction term can be ignored. It is interesting to note that N can never reach N_0 but approaches the maximum that can be electrodeposited ℓN_0 . Therefore unless $\ell = 1$, there will always be some actinium left in solution that is not electrodeposited.

The electrodeposition rate data for this study are given in Table X (p 39) and is used for the calculations in Table XI (p 40). From the data presented, values of 0.987 for ℓ and 0.0686 min^{-1} for ϑ were calculated corresponding to values of $6.77\text{E-}02 \text{ min}^{-1}$ for α and $8.58\text{E-}04 \text{ min}^{-1}$ for β . The relatively low rate of dissolution, β ,

TABLE X
ACTINIUM ELECTRODEPOSITION RATE DATA

Time (min)	N/N ₀	%N/N ₀
0	0	0
15	7.89E-01	78.9%
30	9.25E-01	92.5%
45	9.50E-01	95.0%
60	9.69E-01	96.9%
90	9.79E-01	97.9%
105	9.83E-01	98.3%
165	9.84E-01	98.4%
180	9.87E-01	98.7%

TABLE XI

CALCULATION OF ℓ , θ , AND THE LINEAR VELOCITY CONSTANT κ .

No solution	Activity	atoms	ℓ	θ	alpha	beta	Electrodeposition
uCi 2.93E-01	dps 1.09E+04	1.35E+10	9.87E-01	1/min 0.068554	1/min 6.770E-02	1/min 8.584E-04	min 60
Decay C.F. 0.99712	Buildup C.F. 0.98365	N atoms 1.31E+10	Area cm ² 4.5	Volume mL 15	κ cm/min 2.29E-01	N max atoms 1.34E+10	% Yield 98.08%

compared to α for these experimental conditions suggests that the electrodeposition of ^{225}Ac on the platinum electrode was highly favorable and largely irreversible, as long as the circuit remained closed.

The constant \mathcal{Q} can be written in terms of a linear rate constant κ with units of cm/min. The relationship in terms of κ can be approximated by: $\mathcal{Q} = \kappa \cdot A/V$, where A is the active area of the cathode and V is the volume of solution containing the atoms to be deposited. The rate constant, κ can also be derived as:

$$\kappa = (V/At) \ln(\mathcal{L}N_0 / (\mathcal{L}N_0 - N)).$$

The value of κ for ^{225}Ac on Pt in this study was 0.23 cm/min. This is the first reported data for ^{225}Ac on Pt. Values for κ found in the literature were 0.38 cm/min for Po on Au [32], 0.74 cm/min for ^{210}Po on Ag [33], and 0.77 cm/min for ^{67}Cu on Pt [34]. In view of the different substrates, ions deposited, and electrodeposition conditions (area of electrodes, volume of solution, activity of isotopes, etc.), it is not too surprising to find such a range of values for κ .

CHAPTER VII

THE ATOM RECOIL COLLECTOR (ARC)

Once the actinium has been electrodeposited on the cathode, it is best to let the actinium regain secular equilibrium with its daughters. Then the ^{221}Fr will have the same activity as the ^{225}Ac and the flux of francium atoms to the recoil collector will be known.

The atom recoil collector (ARC) consists of a copper disc ~3 cm in diameter and about 100 μm thick placed 0.5 cm or less from the cathode with a potential difference of 2000 to 5000 volts between them. See Figure 11 (p 43). The voltage was supplied by a 5000V ORTEC 459 bias supply in a Tennelec Minibin with a TC 909 power supply. The recoil atoms are then allowed to accumulate for a period of time to maximize the yield for ^{221}Fr and ^{213}Bi .

The system as described is somewhat like a capacitor. A capacitor consists of two metal plates with a potential difference between them. The dielectric material between the plates can be a vacuum, air, or a solid material such as mica. Over the course of these experiments, all three dielectrics were tried. However, the yields approached the theoretical maxima in air and because this simplified the apparatus and reduced the setup times, the experiments were done in air.

The capacitance C is related to the area of the plate A , the dielectric material, and the distance between the plates, d , by the equation: $C = \epsilon \cdot A/d$, where ϵ is the product of the dielectric constant, K , and the permittivity of free space, ϵ_0 , which has the value of $8.8562\text{E-}12$ farad/m. [35] The dielectric constant, K is 1.0000 for a

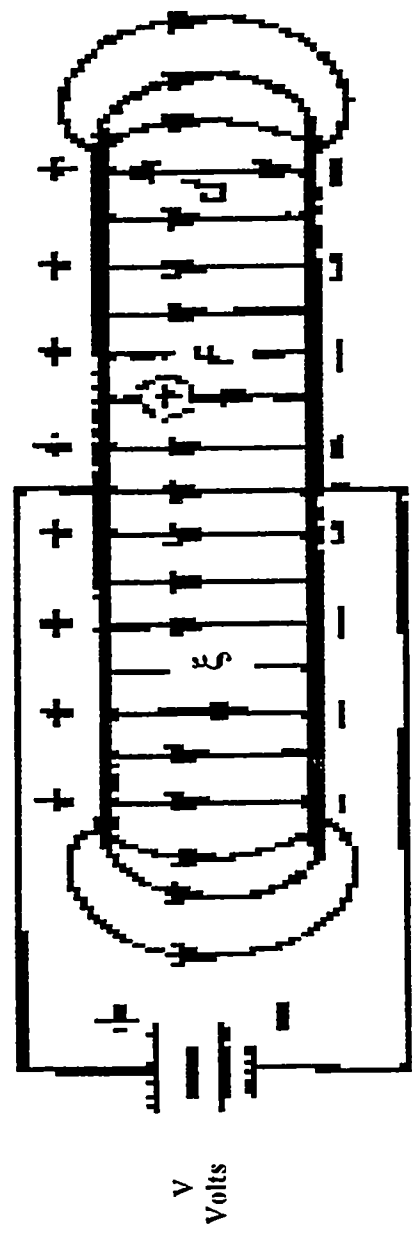


Figure 11. Diagram of atom recoil collector showing lines of force between plates. [35]

vacuum and 1.0006 for dry air. The unit of capacitance is the farad or a subunit thereof, named after Michael Faraday. The average capacitance for the system used here was 1.252 pF.

The capacitance is also related to the total charge, Q , that can be collected on the plates. The relationship is: $C = Q/V$, where V is the potential difference between the plates. This expression also serves as the definition of capacitance as the farad is the number of coulombs per volt. [35]

When a potential difference is placed between two parallel metal plates, the electrostatic field is normal to the plates, uniform, and constant in magnitude and direction over the specified volume of space. [35] Outside the parallel plates and near the boundaries, the electrostatic field is not so uniform. The electrostatic field between the plates, ξ , is given by the equation: $\xi = V/d$, where V is the potential difference between the plates, and d is the distance between them. For example, for a potential difference of 5000 volts and a distance between the plates of 0.5 cm, the electrostatic field would be equal to 1,000,000 V/m. The particles travelling in such a field follow the lines of force between the two parallel plates. [35] See Figure 11 (p 43).

In an electrostatic field ξ between two parallel plates, the force F exerted on a particle of charge q is $F = \xi q$. If the particle is free to accelerate, its kinetic energy $T = qV$. [14] Therefore, the kinetic energy of the particle depends only on its charge and the value of the accelerating potential and is independent of the mass of the particle and the distance it travels in the electrostatic field. [14] Tables XII (p 45) and XIII (p 46) give the forces and kinetic energies of ^{221}Fr and ^{213}Bi , respectively, for three different voltages.

TABLE XII.
 ^{221}Fr ATOM RECOIL COLLECTOR (ARC) CALCULATIONS

Volts (V) negative	Total Charge (Q)	# Charges	E (V/m)	F (Newtons)	W (joules)	Velocity (m/s)	Transit Time (ns)
2000	2.67E-09	1.67E+10	4.00E+05	6.41E-14	3.20E-16	4.14E+04	120.7
3500	4.68E-09	2.92E+10	4.00E+05	6.41E-14	5.61E-16	5.48E+04	91.3
5000	6.68E-09	4.17E+10	4.00E+05	6.41E-14	8.01E-16	6.55E+04	76.4

$q = 1$ assumes Fr^{+1}

TABLE XIII.

 ^{213}Bi ATOM RECOIL COLLECTOR (ARC) CALCULATIONS

Volts (V) negative	Total charge (Q)	# charges	E (V/m)	F (Newtons)	W (joules)	Velocity (m/s)	Transit Time (ns)
2000	2.69E-09	5.59E+09	4.00E+05	6.41E-14	9.61E-16	7.24E+04	69.1
3500	4.68E-09	9.73E+09	4.00E+05	6.41E-14	1.68E-15	9.66E+04	51.7
5000	6.68E-09	1.39E+10	4.00E+05	6.41E-14	2.40E-15	1.15E+05	43.3

$q = 3$ assumes Bi^{+3}

To determine the optimum operating parameters for this system, several experiments were run to determine which voltages, recoil collection times, and distances between plates gave the best yields.

The first set of experiments was to determine the duration of recoil collection that gave the best yield. This was done at a potential difference of 5000 volts and a plate separation of 0.5 cm while varying the recoil collection period.

The results are given in Table XIV (p 48) and plotted in Figure 12 (p 49). The results show that the yield increases for the first 40 minutes and then begins to level off. This is in agreement with the buildup of ^{221}Fr with a half-life of 4.9 minutes. The forty minutes represents about eight half-lives to give 99.6% of maximum buildup.

The second set of experiments was to determine the optimum voltage to use. This was done by collecting recoils on the atom recoil catcher at different voltages but at the same distances and collection times. The distance between the plates used was 0.5 cm, and the duration of recoil collection was 40 minutes. The results are given in Table XV (p 50) and plotted in Figure 13 (p 51). The plot shows the yield increases with voltage up to ~2000 volts. There the yield seemed to reach a plateau and level off. The reason for this may be that the total charge that can be collected on the collector plate is exceeded by the charge flux below ~ 2000 volts. This is because the total charge, $Q = CV$, where V is the voltage and C is the capacitance (which is fixed for a given distance between the plates and area of the collection plate). At the lower voltages, the total charge that can be collected is less than the flux of the charges of the recoil atoms impinging on the collector plate and some atoms are not retained.

TABLE XIV.

YIELD VS. TIME

Applied Potential	Distance, d cm	Recoil Capture Time, min	μCi on ARC		μCi on Cathode		% Yield Fr-221	% Yield Bi-213	Calc (μCi)	
			Fr-221	Bi-213	Fr-221	Bi-213			Fr-221	Bi-213
5000	0.5	2	9.64	23.9	100.5	89.8	9.59	26.6	8.54	8.54
5000	0.5	10	48.8	74.6	180	156	27.1	47.8	44.8	44.8
5000	0.5	20	57.8	87.7	193	111	30.0	79.0	57.7	57.7
5000	0.5	40	41.7	63.7	138	118	30.2	54.0	43.1	43.1
5000	0.5	120	53	91.2	193	111	27.5	82.2	61.0	61.0

-V

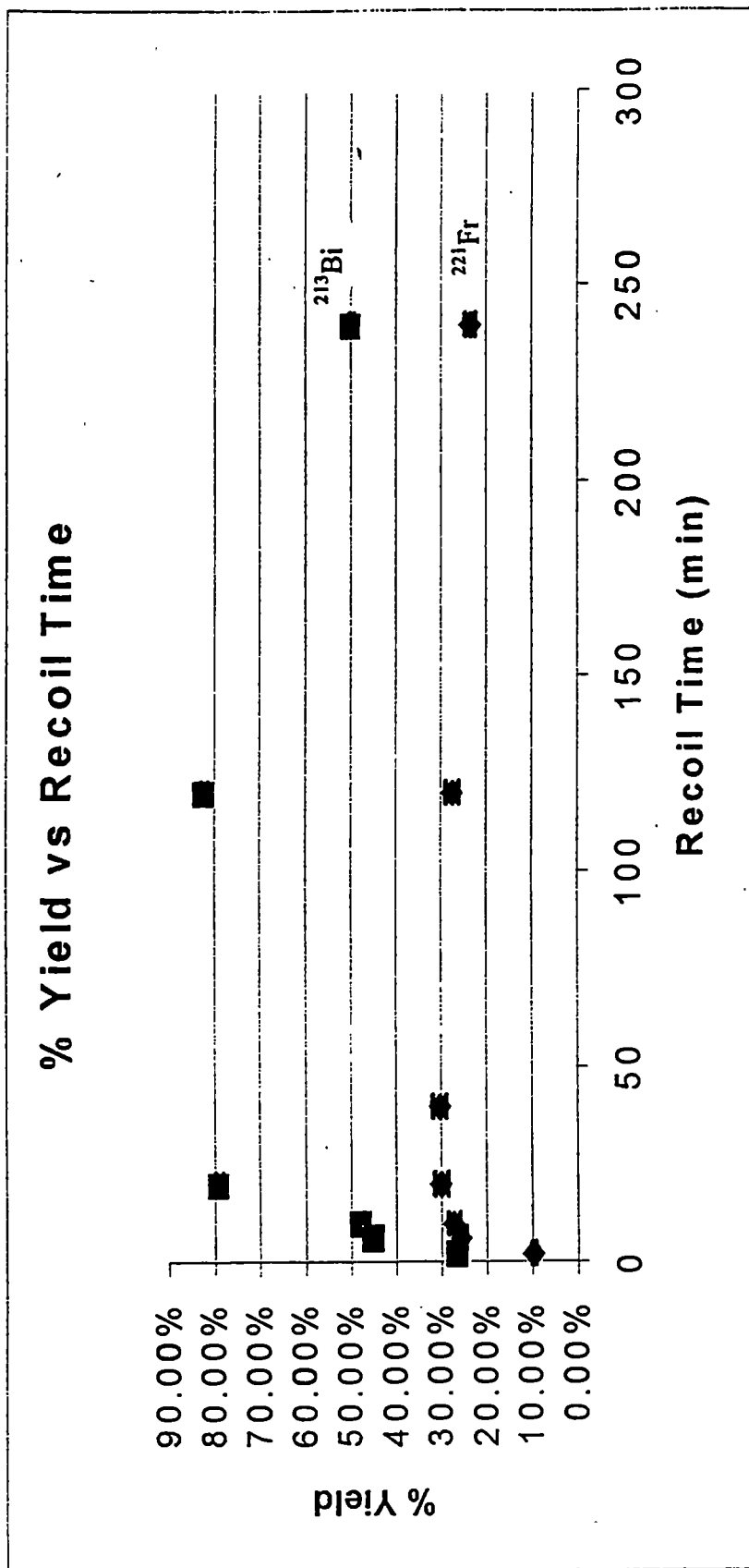


Figure 12. % Yield vs. duration of recoil collection.

TABLE XV
YIELD VS. APPLIED POTENTIAL

Applied Potential -V	Distance, d cm Between Discs	Recoil time, min	μCi on ARC		μCi on Cathode		% Yield Fr-221	% Yield Bi-213	ξ V/m
			Fr-221	Bi-213	Fr-221	Bi-213			
100	0.5	40	28.6	54.9	199.2	177	14.3	31.0	20000
250	0.5	40	31.3	62.7	199.2	177	15.7	35.4	50000
500	0.5	40	32.2	66.2	199.2	177	16.2	37.4	100000
1000	0.5	40	36.4	73.7	199.2	177	18.3	41.6	200000
2000	0.5	40	40.5	61.3	138	118	29.3	51.9	400000
3500	0.5	40	41.4	62.4	138	118	30.0	52.9	700000
5000	0.5	40	41.7	63.7	138	118	30.2	54.0	1000000

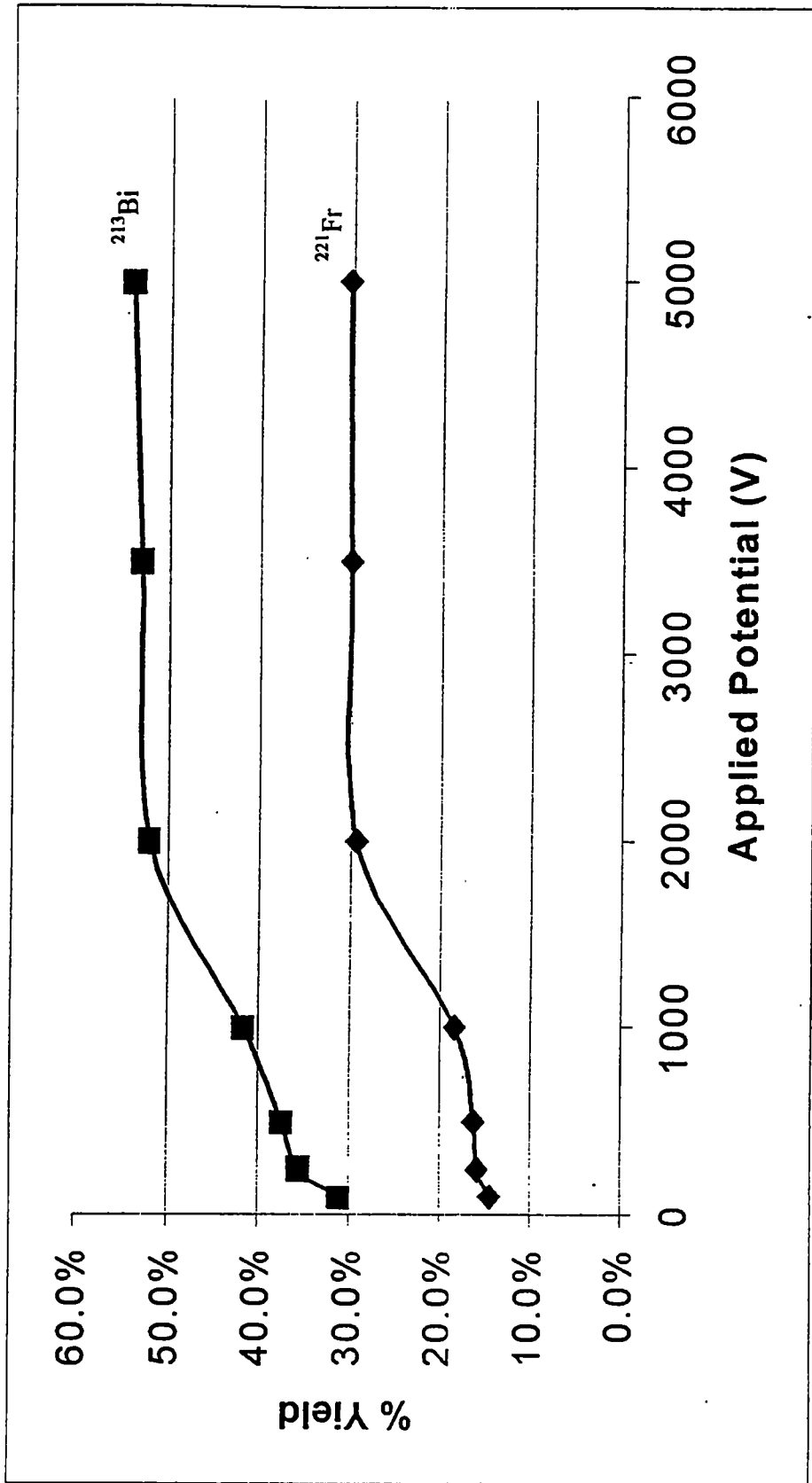


Figure 13. % Yield vs. applied potential.

However, upon reaching a critical voltage, there is enough charge capacity on the collector plate to accommodate all the incoming charges and the yield levels off. This would indicate that the more activity used, the higher the voltage may need to be. However, this trend has not yet been substantiated. Activities used in this study were in the 100 μCi to 200 μCi range. Therefore, for this level of activity, a good operating voltage would be on the plateau around 3000 volts.

During the experiments with different applied potentials, the distance between the plates was kept constant. Therefore, the electrostatic field ξ between the plates varied from 20,000 V/m to 1,000,000 V/m. See values of ξ for different applied potentials in Table XV (p 50).

Another experiment was done to see what effect varying the applied potential but keeping the electrostatic field constant would have on the yields. Table XVI (p 53) and Figure 14 (p 54) show that with the electrostatic field kept constant, the yields do not increase with applied potential but remain constant. Therefore, the yields do not depend on the applied potential but on the electrostatic field intensity. In the earlier experiment, the distances between the plates were kept constant while the applied potential was varied. Therefore, the electrostatic field strength was inadvertently varied, and the yield thus seemed dependent on the applied potential. The data are replotted in Figure 15 (p 55).

The relationship with distance was also investigated. As would be expected, as the distance increased, the yield decreased. See Table XVII (p 53) and Figure 16 (p 57). This follows from the geometry for the angle subtended by the source to the recoil catcher. The geometry correction factor to correct for this is: $f = 0.5(1 - \cos\theta)$, where $\theta = \tan^{-1}(R/d)$, R = the

TABLE XVI
 YIELD VS. CONSTANT ELECTROSTATIC FIELD INTENSITY ($\xi = 1.0E+06$ V/m)

Applied Potential - V	Distance, d cm Between Discs	Recoil Capture time, min	$\mu\text{Ci on ARC}$		$\mu\text{Ci on Cathode}$		% Yield	
			Fr-221	Bi-213	Fr-221	Bi-213	Fr-221	Bi-213
2000	0.2	40	36.6	67.2	158	137	23.2	49.1
3000	0.3	40	36.1	66.0	158	137	22.9	48.2
5000	0.5	40	35.8	65.2	158	137	22.7	47.6

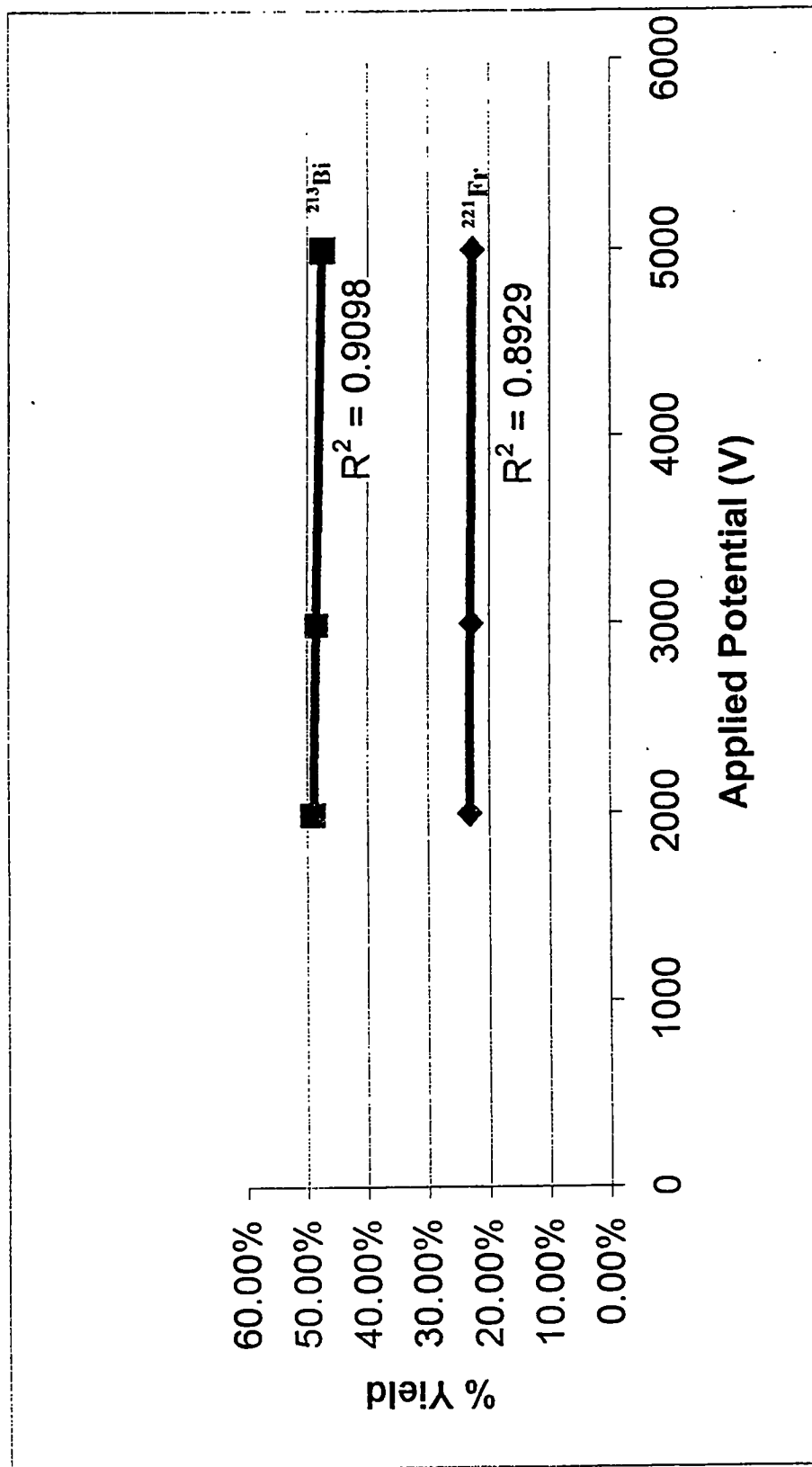


Figure 14. % Yield vs. applied potential at constant ξ ($\xi = 10^6 \text{ V/m}$).

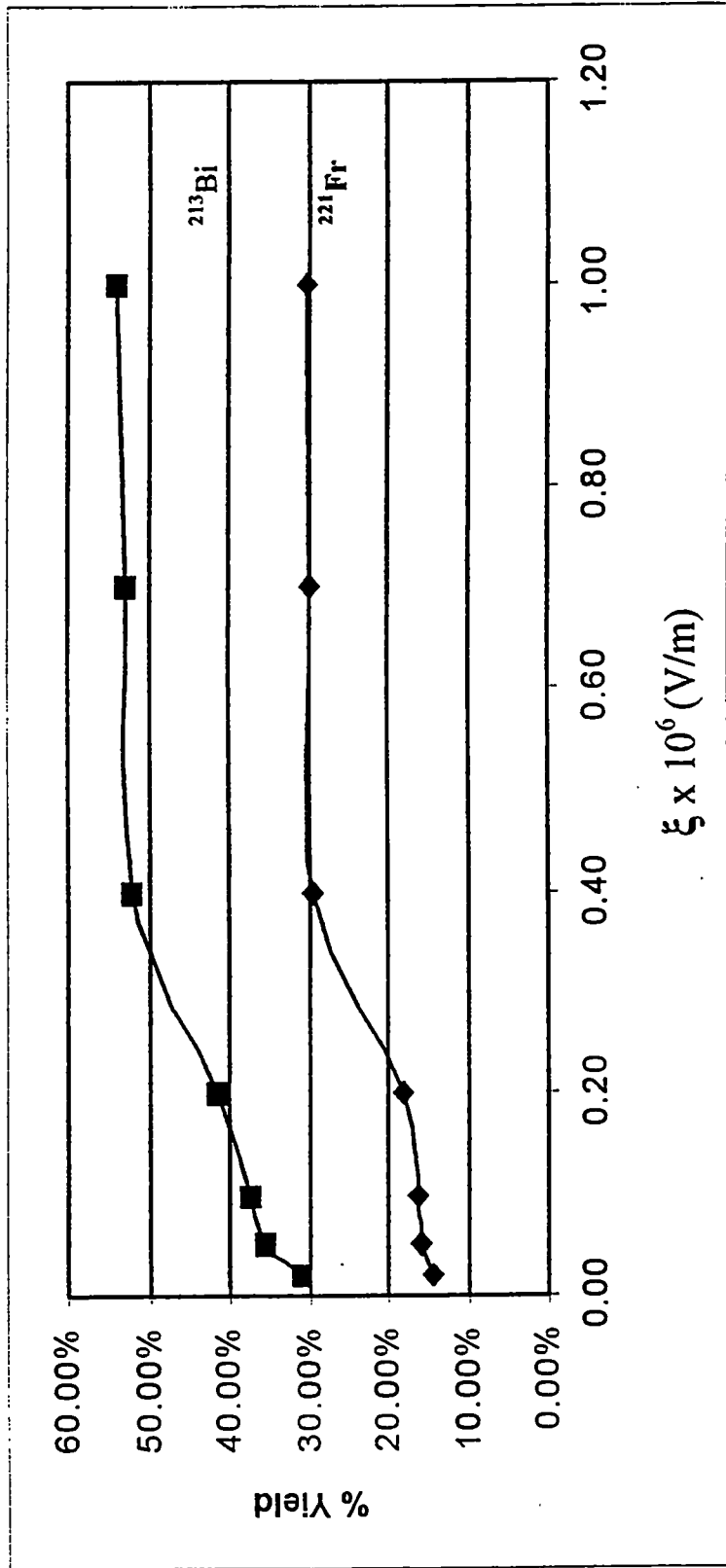


Figure 15. % Yield vs. electrostatic field intensity ξ .

TABLE XVII.
YIELD VS. DISTANCE

Applied Potential - V	Distance, d cm Between Discs	Recoil Capture Time, Min	$\mu\text{Ci on ARC}$		$\mu\text{Ci on Cathode}$		% Yield Fr-221	% Yield Bi-213
			Fr-221	Bi-213	Fr-221	Bi-213		
5000	0.5	40	41.7	63.7	138	118	30.2	54.0
5000	1	40	40.6	60.9	138	118	29.4	51.6
5000	2	40	44.9	82.8	208.6	185	21.5	44.8

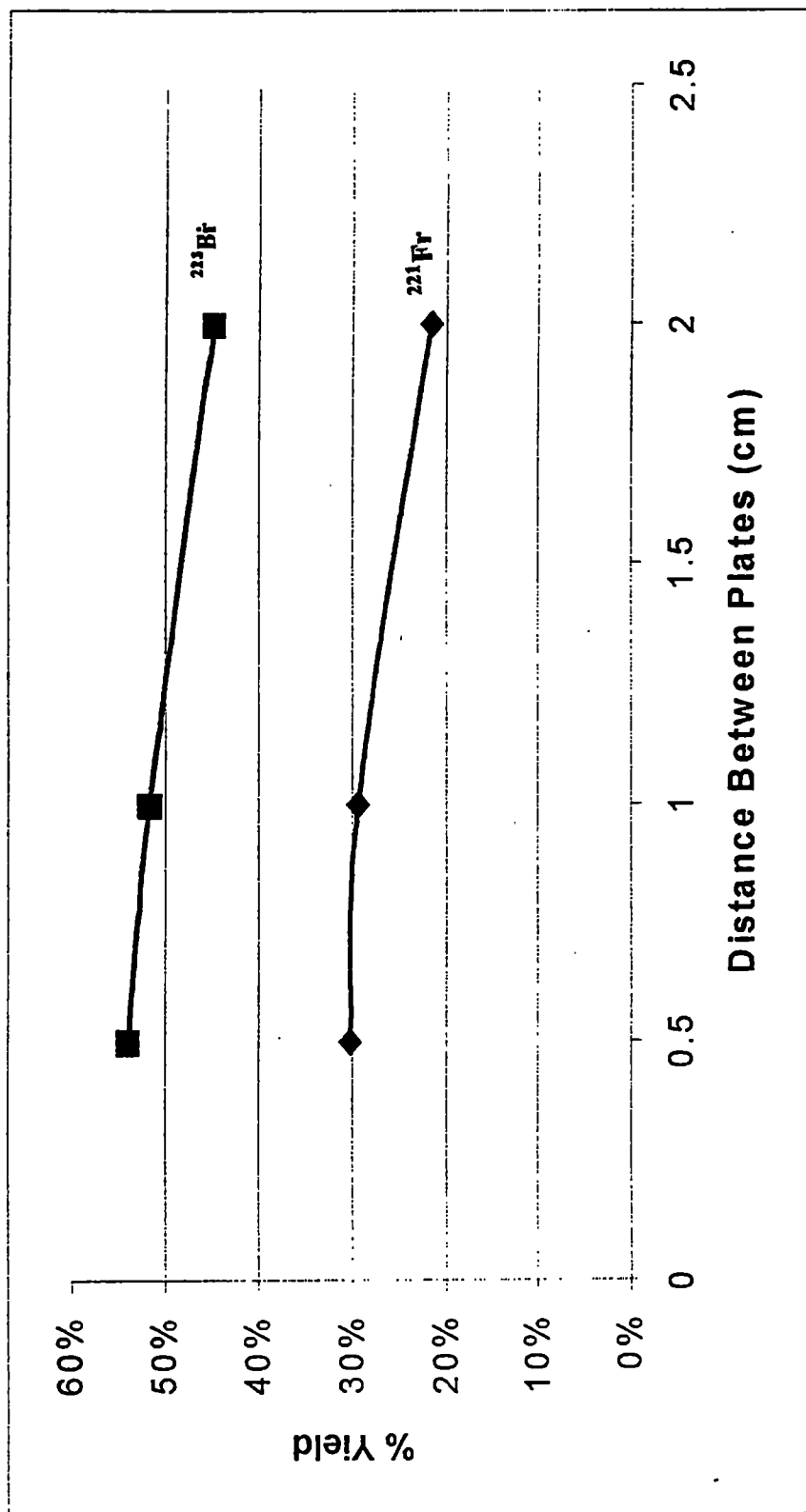
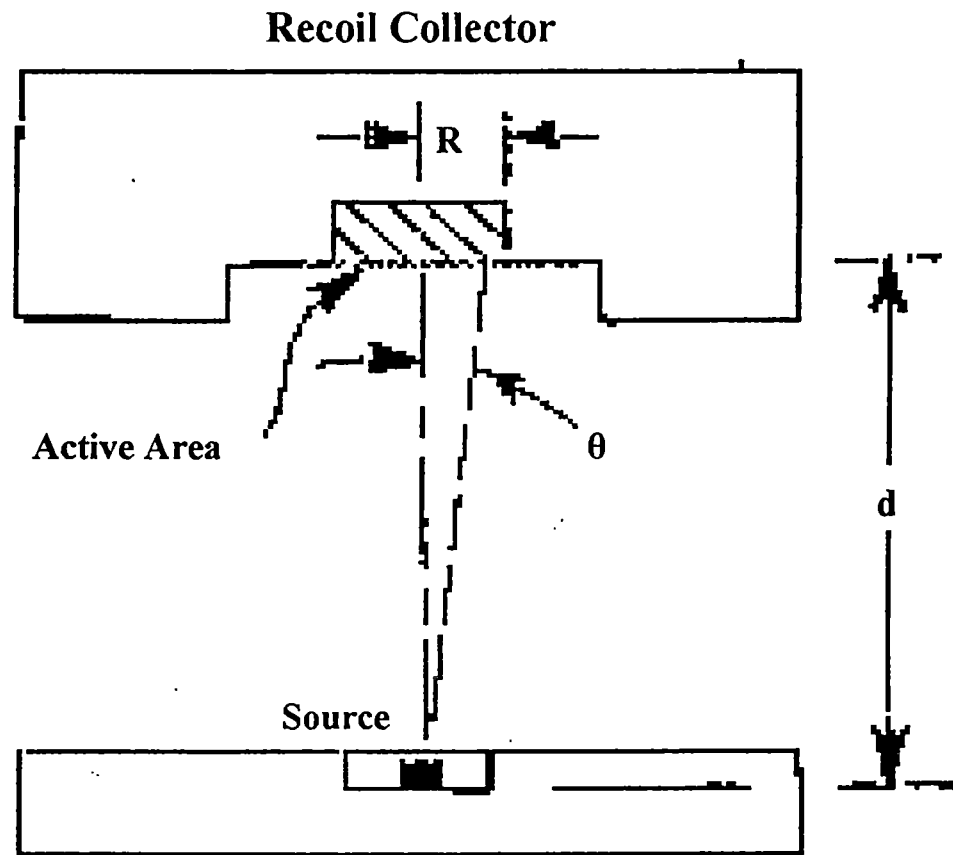


Figure 16. % Yield vs. distance between plates.

the recoil collector, and d = the distance between the recoil collector and the cathode. See Figure 17 (p 59). [32] This equation is analogous to the one used to make geometry corrections for alpha spectroscopy.

A step-by-step procedure for collecting atoms on the recoil catcher is given in Appendix III (p 80). Data from a typical recoil collection are given in Tables XVIII (p 60) and XIX (p 61). Figure 18 (p 62) shows a gamma spectrum at the end of the recoil collection period. Figure 19 (p 63) shows a gamma spectrum after about two half-lives of ^{221}Fr are past, showing the decay of the ^{221}Fr and ^{213}Bi and the absence of ^{225}Ac . However, a count of a recoil collector 18 days after collection, still showed a trace of ^{221}Fr and ^{213}Bi . This indicated a trace of ^{225}Ac was present on the recoil collector. Assuming secular equilibrium and based on the activities of ^{221}Fr and ^{213}Bi measured, a maximum activity of ^{225}Ac of 0.9 nCi was calculated. The ^{225}Ac may be present on the collector because the alpha decay of the ^{221}Fr and ^{213}Bi on the cathode may ionize and dislodge some of the ^{225}Ac atoms in the matrix, thus allowing them to be caught in the electrostatic field and collected. However, the activity of ^{225}Ac inadvertently collected represented less than 0.001% of the original starting activity.



$$f = 0.5(1 - \cos\theta)$$

$$\theta = \tan^{-1}(R/d)$$

Figure 17. Geometry factor diagram. [32]

23-May-88 01:13:50 SP= MCA1/1 OFF CFS 16384/ALin CC 374/ 188.277

3. MARKERS/ROI
 Chans 4896
 LD=1 RD= 1825
 LM=369 RM= 379

CURSOR
 Chan 374
 Cnts 326

TOTALS
 Totl 3630
 Net -48
 Back 3678
 PChan 372
 PCnts 373
 Counts per Sec
 Total 30
 Net 35791393

ROIs Defined 5

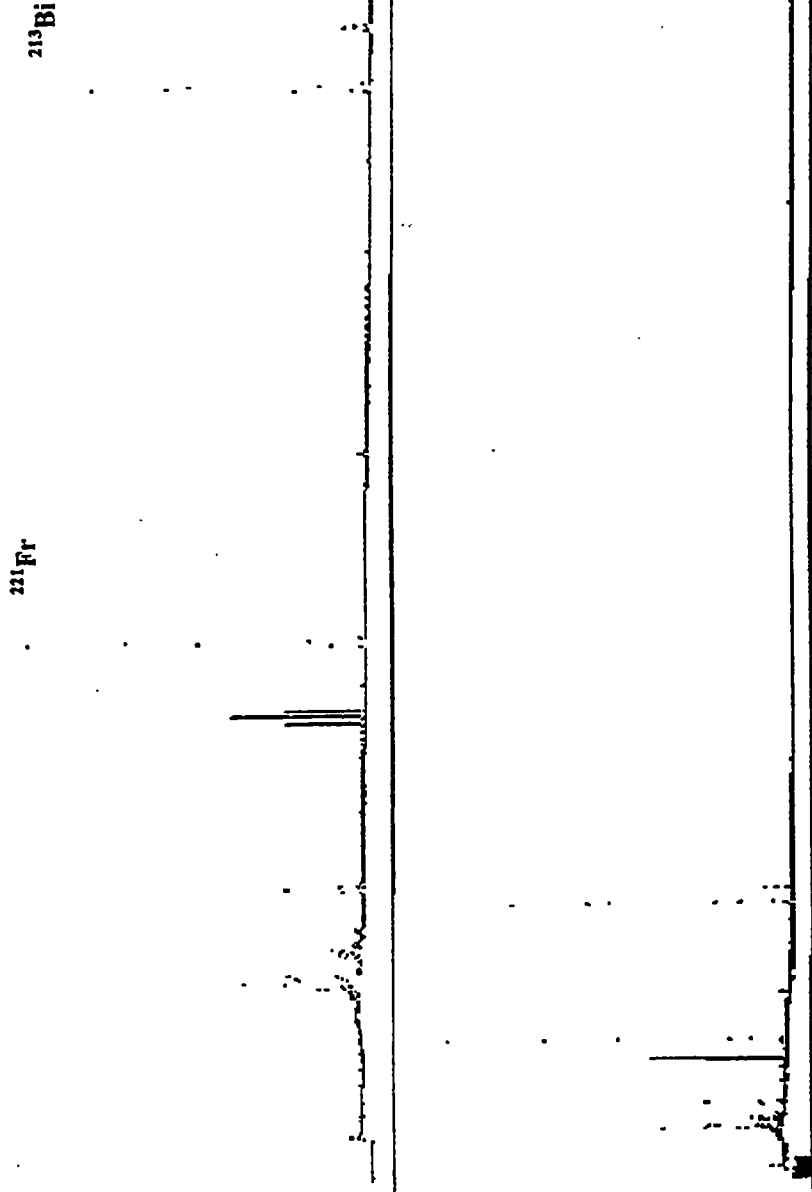


Figure 18. Gamma spectrum of cathode after recoil separation showing and ²¹³Bi collected.

23-May-00 01:21:09 SP= MCA1/1 OFF CFS 32768/ALin CC 374/ 100.277

3. MARKERS/ROI
 Chans 4096
 LD=1 RD= 1025
 LM=867 RM= 881

CURSOR
 Chan 374
 Cnts 749

TOTALS
 Totl 73022
 Net 70755
 Back 2267
 PChan 876
 PCnts 24045
 Counts per Sec
 Total 608
 Net 589

ROIs Defined 5

²¹³Bi

²²¹Fr

Figure 19. Gamma spectrum of cathode after recoil separation showing the absence of ²²⁵Ac and the decay of ²²¹Fr and ²¹³Bi.

CHAPTER VIII

CALCULATION OF ACTIVITIES ON THE RECOIL CATCHER

Once the recoil atoms have been collected, the activity can be quantitated by gamma spectroscopy. However, it would be helpful to calculate the activity of the recoil atoms before the recoil capture is begun.

To do this the chain decay equation is used. It is as follows:

$$A_{Fr} = (\lambda_{Fr}/(\lambda_{Fr} - \lambda_{Ac})) * A_{Ac}^0 * (e^{-\lambda_{Ac} t} - e^{-\lambda_{Fr} t}),$$

where A_{Fr} is the activity of ^{221}Fr at time t , A_{Ac}^0 is the activity of ^{225}Ac at $t = 0$ and λ_{Fr} and λ_{Ac} are the respective decay constants. However, because the ^{221}Fr activity has been moved through space by the recoil action, the chain decay equation must be multiplied by the geometry factor f as given in the previous chapter. The new equation then becomes:

$$A_{Fr} = (\lambda_{Fr}/(\lambda_{Fr} - \lambda_{Ac})) * A_{Ac}^0 * f * (e^{-\lambda_{Ac} t} - e^{-\lambda_{Fr} t}).$$

When the chain decay equation is multiplied by this geometry factor, the calculated activity agrees well with the measured activity of ^{221}Fr on the recoil collector. In the special case of secular equilibrium when the half-life of the parent is much, much longer than the half-life of the daughter, the above equation reduces to:

$$A_{Fr} = A_{Ac} * f.$$

Figure 20 (p 65) shows the relationship between the calculated and measured activities of ^{221}Fr to be linear with an R^2 of 96%. The R^2 means that 96% of the variation in the data is accounted for in this linear model.

Since f is a function of the radius of the collector and the distance between the plates, these variables can be adjusted to give the desired activity of ^{221}Fr to be collected.

This equation does not hold for ^{213}Bi however. On the recoil collector, the ^{213}Bi collected is from the ^{221}Fr that decays on the collector as well as the collection of ^{213}Bi recoils from the source itself. Another factor is the intermediate short-lived daughter of ^{221}Fr , ^{217}At ($t_{1/2} = 32$ milliseconds), which decays to ^{213}Bi . When it decays on the collector, some of the ^{213}Bi atoms will be ejected from the collector. Some may be returned by the electrostatic field, but some will be lost as well. Therefore, a suitable equation for the production of ^{213}Bi is complex and has yet to be worked out satisfactorily.

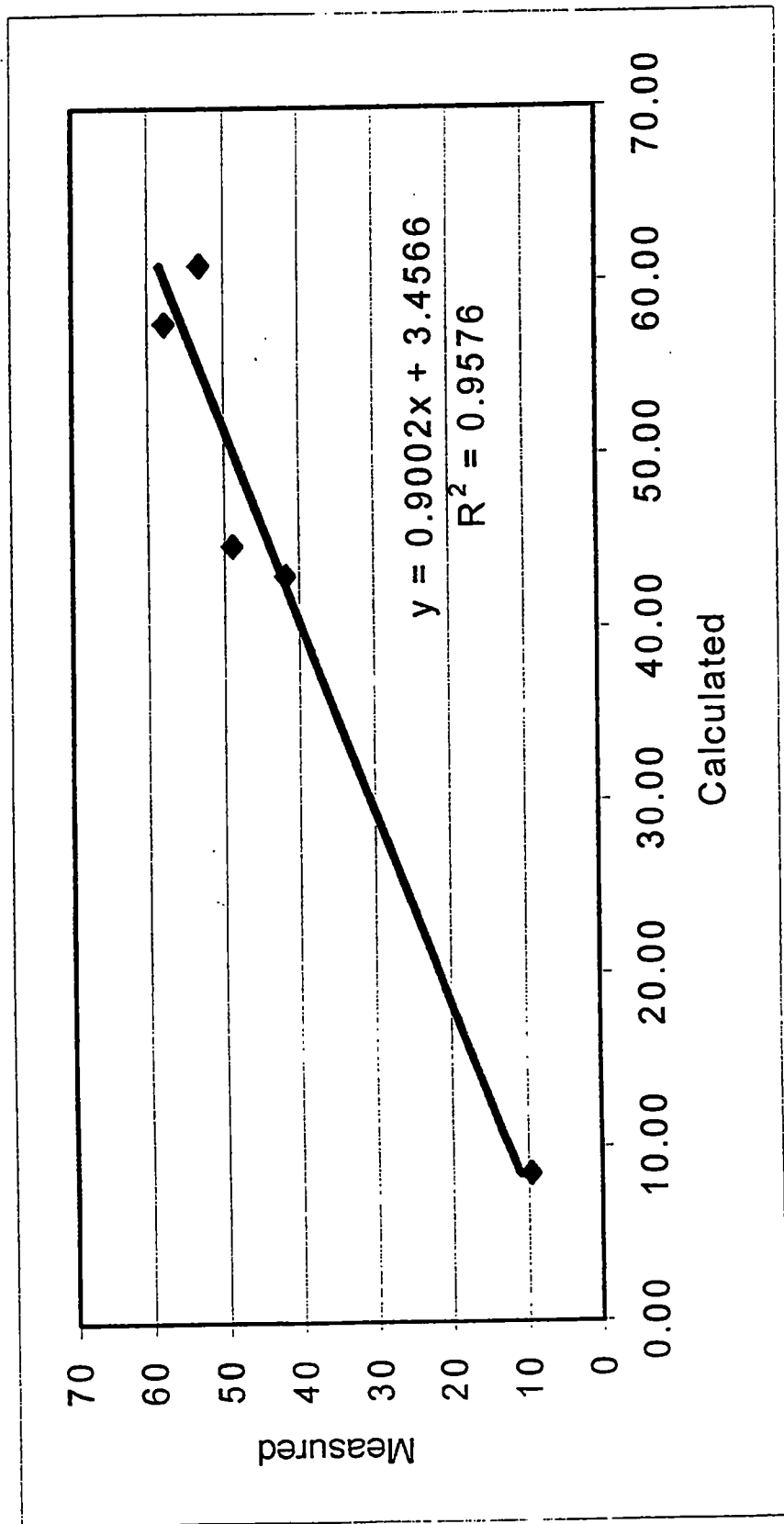


Figure 20. ^{221}Fr Activity Measured vs. Calculated.

CHAPTER IX

FUTURE WORK

As with any study, there are always more questions to be answered. One of the most pressing questions is what is the best method to remove the ^{221}Fr and ^{213}Bi from the recoil catcher. In this study, copper was used, but it was found that the radioactivity could not be removed by dipping in dilute to concentrated hydrochloric or nitric acids. It was also observed that alpha activity could be detected on the side of the copper disc away from the cathode. It is not certain whether this activity was due to "alpha creep," ^{217}Rn which is a minor decay branch of ^{217}At (0.01%), or if some of the ^{221}Fr and ^{213}Bi atoms had sufficient momentum, due to the electrostatic field, to penetrate the thickness of the copper disc. This last alternative seems unlikely due to the thickness of the disc of $\sim 100\ \mu\text{m}$ (see Table VI p 21). It is clear though that some of the activity is imbedded in the copper and is not on the surface where it can be easily removed. To keep the francium and bismuth from being imbedded in the copper, a material of atomic weight greater than that of francium and bismuth is required. However, all the elements above francium and bismuth are radioactive and could pose a further contamination problem either from themselves or from their daughters. A possible solution would be an alloy of freshly separated uranium that could stop the recoil atoms from penetrating and yet not be a source of other contamination. Another factor to consider is the increase in elastic scattering a heavier element would cause with a corresponding decrease in the yield. However, there

should be some tradeoff between hardness and elastic scattering that could be achieved.

A better solution may be to find a film of some material that would coat the copper and on which the recoil atoms would deposit. The film would then be removed and the recoil atoms with it. Then the film could be dissolved to liberate the recoil atoms without any copper contamination.

Another possibility would be to find a suitable chelating agent to extract the recoil atoms from the copper that would not dissolve the copper. This may be possible if the thickness of the copper is not too great.

A final possibility would be to completely dissolve the copper and then extract it or the recoil atoms from the other by ion exchange or some other method. However, the process would need to be quick due to the short half-lives of the isotopes involved.

Once a suitable material for the collection disc has been found, the separation of other isotopes may be tried. One possible candidate may be ^{224}Ra from ^{228}Th . The collection times would need to be longer due to the longer half-lives but the recoil collection would be feasible.

Another useful result to have would be the mathematical expression for calculating the activity of ^{213}Bi on the recoil catcher. This would aid in the production of ^{213}Bi for other laboratory experiments.

Another extension of this technique would be to beta emitters. While the recoil of the daughter atom is not great, it does recoil with maximum recoil energy

RE_{\max} of:

$$RE_{\max}(\text{eV}) = 537E_{\beta}(E_{\beta} + 1.02)/M,$$

where E_{β} is the maximum β energy in MeV and M is the mass of the parent. [11] This is a maximum energy because the recoil energy is dependent on how the kinetic energy of the beta particle is shared with the antineutrino and on the angular correlation between the two particles. [11] For example a 0.5 MeV β decay in a mass 225 nucleus will produce a maximum recoil energy of ~ 1.8 eV. Although small in energy, it is enough to break some chemical bonds, and once the recoil atom is “caught” in the electrostatic field, the field will accelerate it to the collector. Some possible candidates of interest would be ^{225}Ac from ^{225}Ra , ^{210}Bi from ^{210}Pb , ^{227}Th from ^{227}Ac , and ^{212}Bi from ^{212}Pb . Each pair would be a challenge due to nuances in their half-lives, but they would be interesting to try.

Another topic to pursue would be to use the recoil atom flux as a “beam” of atoms to bombard a target of interest. This low (compared to reactor or particle accelerator) flux might prove ideal for putting atoms inside of fullerenes. One experiment suggested would be to coat the collector disc with fullerenes and then bombard them with recoil atoms to see if these atoms could be placed inside the cages. [37] This would be a very interesting and useful application of this technique if it is successful.

CHAPTER X

SUMMARY AND CONCLUSIONS

In summary, the electrostatic collection of recoil atoms has been shown a viable means to separate ^{221}Fr and ^{213}Bi from ^{225}Ac . Yields as high as 50% for ^{221}Fr and 98% for ^{213}Bi have been obtained.

The electrodeposition of ^{225}Ac has been quantitated and shown to obey the Joliot Equation. Deposition and linear velocity constants for actinium have been calculated.

The atom recoil catcher system has been studied to determine its optimum parameters. It was found that the yields are dependent on the strength of the electrostatic field and the distance between the plates. It was further found that the yield increased with electrostatic field strength but leveled off after a critical voltage had been reached. The length of time for optimum buildup of ^{221}Fr on the collector was found to be 40 minutes.

An equation has been identified for the calculation of ^{221}Fr activity on the recoil collector. Knowing the source activity, area of the recoil collector, and the distance between the plates, the activity of the ^{221}Fr collected can be calculated in advance. Conversely, knowing the amount of activity to be collected can be used as input to determine the experimental parameters.

Finally, ^{221}Fr and ^{213}Bi can be separated from ^{225}Ac by electrostatic collection of the recoil atoms in high yield and without the usual problems and wastes generated by the normal means of ion exchange separation.

LIST OF REFERENCES

LIST OF REFERENCES

1. Malkemus, D., "Vapor Extraction of an $^{225}\text{Ac}/^{213}\text{Bi}$ generator," Master's Thesis, University of Tennessee, Knoxville, 1999.
2. Gould, H., University of California, Berkeley, Personal communication, 1997.
3. McDevitt, M. R., G. Sgouros, R. D. Finn, J. L. Humm, J. G. Jurcic, S. M. Larson, D. A. Scheinberg, "Radioimmunotherapy with Alpha-emitting Nuclides," *European Journal of Nuclear Medicine*, Vol.25, No. 9, pp.1341-1351, 1998.
4. Knapp, Jr., F. F., S. Mirzadeh, "The Continuing Important Role of Radionuclide Generator Systems for Nuclear Medicine," *European Journal of Nuclear Medicine*, Vol. 20, No. 12, pp. 1151-1165, 1994.
5. Sgouros, G., A. M. Ballangrud, J. G. Jurcic, M. R. McDevitt, J. L. Humm, Y. E. Erdi, B. M. Mehta, R. D. Finn, S. M. Larson, D. A. Scheinberg, "Pharmacokinetics and Dosimetry of an α -Particle Emitter Labeled Antibody: ^{213}Bi -HuM195 (Anti-CD33) in Patients with Leukemia," *The Journal of Nuclear Medicine* Vol. 40, No.11, pp.1935-1946, 1999.
6. Scheinberg, D. A., et al., "Alpha Particle Therapy for Cancer", Symposium on Radioisotope in Medicine: New Promise for the Treatment of Cancer, Seattle, WA, February 15, 1997.
7. Boll, R. A., S. Mirzadeh, S. J. Kennel, D. W. DePaoli, and O. F. Webb, "Bi-213 for Alpha-particle-mediated Radioimmunotherapy", XII International Symposium on Radiopharmaceutical Chemistry, Uppsala, Sweden, June 15-19, 1997.
8. Mirzadeh, S., "Generator-produced Alpha-emitters," *Appl. Radiat. Isot.*, Vol. 49, No. 4, pp. 345-349, 1998.

9. Boll, R. A., S. Mirzadeh, and S. J. Kennel, "Optimization of Radiolabeling of Immunoproteins with ^{213}Bi ," *Radiochimica Acta*, Vol. 79, pp. 145-149, 1997.
10. Gmelin Handbook of Inorganic Chemistry, Actinium Supplement Volume 1, 8th Edition, pp.104-107; 115; 207-209; 223, 225, Springer-Verlag, New York, 1981.
11. Friedlander, G., J. W. Kennedy, E. S. Macias, J. M. Miller, Nuclear and Radiochemistry, 3rd Edition; pp.206-243 and p.438, John Wiley and Sons, New York, NY, 1981.
12. Radiological Health Handbook, Bureau of Radiological Health, Public Health Service, U. S. Department of Health, Education, and Welfare, Rockville, MD, January 1970.
13. Browne, E., R. B. Firestone, Table of Radioactive Isotopes, pp. 225-1, 221-2, 213-1, John Wiley & Sons, New York, 1986.
14. Rutherford, E., "Radioactivity Produced in Substances by the Action of Thorium Compounds," *The London, Edinburgh, and Dublin Philosophical Magazine and Journal of Science* [5], 49, pp.161-192, 1900 as reprinted in The Discovery of Radioactivity and Transmutation, Edited by Alfred Romer, pp.38-69, Dover Publications, Inc., New York, 1964.
15. Meinke, W. W., A. Ghiorso, and G. T. Seaborg, "Artificial Chains Collateral to the Heavy Radioactive Families," *Physical Review*, Vol. 81, No. 5, pp. 782-798, 1951.
16. Meinke, W. W., A. Ghiorso, and G. T. Seaborg, "Further Work on Heavy Collateral Radioactive Chains," *Physical Review*, Vol. 85, No. 3, pp. 429-431, 1952.
17. Ghiorso, A., T. Sikkeland, J. R. Walton, and G. T. Seaborg, "Attempts to Confirm the Existence of the 10-Minute Isotope of 102." *Physical Review Letters*, Vol. 1, No. 1, pp. 17-18, 1958.
18. Ghiorso, A., T. Sikkeland, J. R. Walton, and G. T. Seaborg, "Element No. 102." *Physical Review Letters*, Vol. 1, No. 1, pp. 18-21, 1958.

19. Ghiorso, A., T. Sikkeland, A. E. Larsh, and R. M. Latimer, "New Element, Lawrencium, Atomic Number 103." *Physical Review Letters*, Vol. 6, No. 9, pp. 473-475, 1961.
20. MacFarlane, R. D., and R. D. Griffioen, "A System for Studying Accelerator-Produced Short-Lived Alpha Emitters," *Nuclear Instruments and Methods*, Vol. 24, p. 461, 1963.
21. Valli, K., W. J. Treytl, and E. K. Hyde, "On-Line Alpha Spectroscopy of Neutron-Deficient Actinium Isotopes," *Physical Review*, Vol. 167, No. 4, pp. 1094-1104, 1968.
22. Dinneen, T., A. Ghiorso, and H. Gould, "An Orthotropic Source of Thermal Atoms," *Review of Scientific Instruments*, Vol. 67, p. 752, 1996. LBL 37439-REV.
23. Lu, Z.-T., K. L. Corwin, K. R. Vogel, C. E. Wieman, T. P. Dinneen, J. Maddi, and H. Gould, "Efficient Collection of ^{221}Fr into a Vapor Cell Magneto-optical Trap," *Physical Review Letters*, Vol. 79, No. 6, pp. 994-997, 1997.
24. Kouassi, M. C., J. Dalmasso, H. Maria, G. Ardisson, M. Hussonnois, "On the γ -Spectrum Following ^{225}Ac α -Decay," *J. Radioanal. Nucl. Chem. Letters*, Vol. 144, No. 5, pp. 387-396, 1990.
25. EM Science Omnitrace Nitric Acid, Assay 69.8%, Lot No. NX0407-1.
26. Harvey, B. G., *Introduction to Nuclear Physics and Chemistry*, 2nd Edition, pp. 327-328, 364, Prentice-Hall, Inc., New Jersey, 1969.
27. National Nuclear Data Center, "Nuclear Wallet Cards," 6th Edition, Brookhaven National Laboratory, Upton, NY, January 2000.
28. Mueller, W. A., *Radiochim. Acta*, Vol. 9, pp. 181-186, 1968.

29. Rane, A. T. and K. S. Bhatki, "Electrodeposition of Carrier-Free Manganese-54, Technetium-99, and Actinium-228 from Aqueous Baths," *International Journal of Applied Radiation and Isotopes*, Vol. 24, pp. 385–389, 1973.
30. Iyer, R. H., H. C. Jain, M. V. Ramaniah, and C. L. Rao, "Electrodeposition of Actinium," *Radiochim. Acta*, Vol. 3, p.225, 1964.
31. Joliot, F., "Étude Electrochimique des RadioÉléments: Applications Diverses," *J. Chim. Phys.*, Tome 27, pp. 1930.
32. Fahland, J., G. Herrmann, and F. Strassmann, "Zur Kinetik der Elektrochemischen Abscheidung Radioaktiver Ionenarten auf Metalloberflächen," *J. Inorg. Nucl. Chem.*, Vol. 7, pp. 201–209, 1958.
33. Reischmann, F. -J., B. Rumler, N. Trautmann, and G. Herrmann, "Chemistry at Low Concentrations: Polonium at a Level of 5000 to 40 Atoms," *Radiochimica Acta*, Vol. 39, pp. 185-188, 1986.
34. Mirzadeh, S., and F. F. Knapp, Jr., "Spontaneous Electrochemical Separation of Carrier-free Copper-64 and Copper-67 from Zinc Targets," *Radiochimica Acta*, Vol. 57, pp. 193–199, 1992.
35. White, H. E., Modern College Physics, 6th Edition, pp. 361–373, D. Van Nostrand Company, New York, 1972.
36. Spectrometry Experiments with Multichannel Analyzers, The Nucleus, Inc., pp. 40–41, 1981.
37. Mirzadeh, S., Oak Ridge National Laboratory, private communication, 2000.

APPENDICES

APPENDIX I

Source Solution Preparation

1. Rinse a 20 mL liquid scintillation vial with 0.01 M nitric acid.
2. Add ~ 5 mL of 0.01 M nitric acid to the vial.
3. Quantitatively transfer ~ 200 μL of ^{225}Ac stock solution in 0.1 M nitric acid to the 20 mL scintillation vial with 10 mL of 0.01 M nitric acid. pH should be about 1.6.
4. Add a magnetic stir bar and place cap on vial.
5. Stir on low (settings 3 or 4) for at least 10 minutes until well mixed.
6. Count source solution on a HPGe detector.

APPENDIX II

Electrodeposition Procedure

1. The platinum cathode should be $\sim 1.5 \times 1.5$ cm square arc welded to a Pt wire ~ 5 cm long. The anode consists of only a Pt wire ~ 5 cm long.
2. Wash the electrodes in conc. nitric acid. Rinse with DI water and blot dry.
3. Place electrodes in solution ~ 0.5 cm apart.
4. Hook negative terminal of the DC power supply to the cathode and the positive to the anode.
5. Turn voltage to 8 volts and monitor the current during the electrolysis. Record ammeter readings at beginning and at the end of the electrodeposition.
6. Add 0.01 M HNO_3 if necessary to keep electrodes covered.
7. Allow the electrodeposition to proceed for 1 hour.
8. At the end of 1 hour, take the cathode out of the solution with the voltage still on. Be careful not to touch the electrodes together. Record time of cathode removal.
9. Turn off the voltage.
10. Rinse cathode with DI water to wash off the acid and carefully blot dry.
11. Count the 20 mL vial solution again on an HPGe detector for 2 minutes. Record time of count start.

APPENDIX III

Atom Recoil Collection (ARC) Procedure

1. Put the cathode from the previous electrodeposition in the cathode holder and count on an HPGe detector for 2 minutes. Record time of count start.
2. When count is completed, attach cathode to the positive or ground terminal of the recoil catcher apparatus.
3. Attach the copper disc collector to the negative terminal of the atom recoil catcher (ARC) apparatus to catch the positive ions.
4. Turn high voltage to -3000 volts. Record time voltage on.
5. Accumulate recoils for 40 minutes.
6. Turn high voltage off. Record time voltage off.
7. Unhook cathode and put away for future use.
8. Unhook the copper disc collector from the recoil catcher apparatus.
9. Count the disc collector on an HPGe detector for 2 minutes. Due to the amount of activity collected, the disc may need to be counted at 10 cm or more from the detector. Record time of count start.
10. Enter data into a spreadsheet and calculate % yield.

VITA

John Daniel Marsh, Jr. was born in Richmond, Virginia on September 9, 1953. He graduated from Gloucester High School in June 1971 and then attended the University of Richmond. He graduated there in May 1976 with a B.S. in Chemistry and minors in Physics, Mathematics, and Biology. The summer before graduation, he worked at the Virginia Division of Consolidated Laboratory Services in Richmond, Virginia where he analyzed meat for fat content. After graduation, he married Margaret (Peggy) Archer Green and moved to Gainesville, Florida where he had accepted a job with Environmental Science & Engineering, Inc. There he had his first introduction to Radiochemistry, the analysis of ^{226}Ra in water samples by the Radon Deemanation Method, and learned his way around the counting room. After three years at ESE, he attended the University of Florida in Gainesville and earned a M.S. in environmental radiochemistry under Dr. Emmett Bolch in the Environmental Engineering Sciences Department. While there, he had an assistantship analyzing environmental samples for the Crystal River Nuclear Power Plant. After graduation, he accepted a civilian job with the United States Air Force at McClellan Air Force Base in Sacramento, California. There he worked as a nuclear scientist in support of monitoring the 1963 Nuclear Test Ban Treaty on Atmospheric Testing. In 1987, he accepted a position at Oak Ridge National Laboratory (ORNL) with the Environmental Sciences Division. There he studied the migration of radioisotopes from the burial grounds into the environment and presented several papers at national meetings of the American Chemical Society of which he is a member. While at ORNL he began to work part time on his Ph.D. in chemistry at

the University of Tennessee, Knoxville. In 1996, he moved to the K-25 Site to provide his gamma spectroscopy expertise to the Nondestructive Assay (NDA) Department. In 1997, he began his research in the Nuclear Medicine Group at ORNL and in 1999, he joined the staff of Canberra Industries continuing his NDA work.

The author continues to live in Oak Ridge with his wife and five children where he serves on the Board of Directors of the Wesley Woods Environmental Camp, is a member of First United Methodist Church and is an Assistant Scoutmaster of Troop 129.